Effective Hamiltonian for liquid-vapor interfaces

K. R. Mecke and S. Dietrich
Fachbereich Physik, Bergische Universität Wuppertal, D-42097 Wuppertal, Federal Republic of Germany
(Received 11 January 1999)

Starting from a density functional theory for inhomogeneous fluids we derive an effective Hamiltonian for liquid-vapor interfaces of simple fluids which goes beyond the common phenomenological capillary-wave description. In contrast to other approaches we take into account the long-ranged power-law decay of the dispersion forces between the fluid particles which changes the functional form of the wave-vector-dependent surface tension qualitatively. In particular, we find two different forms of the bending rigidity for the capillary waves, a negative one for small wave vectors determined by the long-ranged dispersion forces and a positive rigidity for large wave vectors due to the distortions of the intrinsic density profile in the vicinity of the locally curved interface. The differences to the standard capillary-wave theory and the relevance of these results for the interpretation of scattering experiments are discussed. [S1063-651X(99)10406-9]

PACS number(s): 68.10.−m, 82.65.Dp, 61.25.Bi

I. INTRODUCTION

The distinction between the liquid phase and the vapor phase of a given substance is facilitated only by bringing them into spatial contact under appropriate thermodynamic conditions so that a liquid-vapor interface can form. In spite of this significant conceptual and practical importance the structural properties of fluid interfaces are still unresolved due to the dearth of rigorous theoretical results for realistic systems in spatial dimensions $d=3$ [1–3]. The reason for this uncomfortable situation is the fact that at fluid interfaces two types of fluctuations occur simultaneously which require both the same careful statistical analysis: (i) fluctuations in the bulk, which are present also in the absence of the interface and cause, e.g., the temperature dependence of the fluid densities, and (ii) capillary waves of the interface position. Whereas the spatial extension of the bulk fluctuations varies between the molecular diameter r_0 of the species and the bulk correlation length ξ, the wavelengths of the capillary waves span the range between ξ and the capillary length $l_c = \sqrt{\sigma/(\Delta\rho m G)}$ where σ is the macroscopic surface tension, $\Delta\rho=\rho_l-\rho_g$ the difference between the number densities of the liquid and vapor phase, respectively, m the mass of the species, and G the gravitational constant.

In view of the absence of rigorous results the structure of fluid interfaces has been investigated by approximate schemes. To this end two approaches have emerged. The first one, developed originally by van der Waals (vdW) [4], introduces a laterally flat intrinsic density profile across the interface interpolating smoothly between the densities of the bulk phases. The second approach, put forward by Buff, Lovett, and Stillinger (BLS) [5], describes the actual smooth profile as the thermal average of a fluctuating steplike interface between the phases. The main difference between the two approaches resides in the assumption what the relevant fluctuations are. Whereas the van der Waals theory identifies the density fluctuations in the bulk phases as the relevant mechanism for the formation of a smooth profile, the complementary BLS approach invokes the capillary waves (CW's) of the interface, which have no counterpart in the bulk.

At low temperatures, i.e., far below the critical point of the two coexisting bulk phases, the intrinsic thickness of the interface is of the size of the particles and the dominant fluctuations are capillary waves which are promoted entropically but opposed by gravity and by the surface tension which penalizes the increase of the interfacial area generated by the capillary waves. Upon raising the temperature the density fluctuations in the bulk phases become more and more important, yielding an intrinsic interfacial thickness proportional to the increasing bulk correlation length. Thus a consistent picture of the fluid interface, in particular for critical phenomena [6], should be one which includes both approaches and clarifies the crossover from one to the other.

In an effort to reconcile the two approaches one may argue that the CW theory describes fluctuations of the interface larger than the bulk correlation length ξ whereas the van der Waals theory takes into account fluctuations below this scale, yielding a smooth density profile [7,8]. In this picture the VdW theory provides a smooth planar interface, the so-called intrinsic interface, whose undulations are described by the CW theory. Although this view is appealing, it suffers from the problem of specifying the length scale which separates both regimes. This length scale is expected to be proportional to the bulk correlation length. However, there is no algorithm which would lead to an accurate determination of this length scale. In addition to this uncomfortable quantitative ambiguity this unified approach is burdened by a more fundamental problem, which is the identification of the fluctuations which are dominant in either regime. One has to ensure that one does not count fluctuations twice, i.e., as contributions to the intrinsic density profile and as capillary waves. Furthermore, this unified approach neglects bulk density fluctuations at scales larger than the correlation length, for which only capillary waves are taken into account. The CW approach does not allow one to take into account bulk density fluctuations which are well separated from the interface, i.e., bubbles on scales larger than the correlation length.

It seems that a more consistent way of reconciling the two approaches consists of distinguishing the different types of fluctuations at all length scales, i.e., for both the undulations of the interface and the bulk density fluctuations. This means

that the intrinsic density profile should take into account only bulk fluctuations but no undulations of the interface position, which are described in a second step by a statistical theory for capillary waves on all scales even for wave vectors larger than the inverse correlation length.

To this end we start from a microscopic density functional theory for inhomogeneous simple fluids, which is a successful approach for the description of nonuniform fluids [9]. We separate the different kinds of density fluctuations—bulk bubbles and interface undulations—by determining the intrinsic density profile via minimizing the functional under the constraint of a locally prescribed interface position; i.e., the location of the isodensity contour of the mean density is given as a function of the lateral coordinates. Thus, by construction the profile does not take into account fluctuations of the interface position. In the second step the complete structure of the interface is obtained by weighting the unfreezing of these interface fluctuations by the cost in free energy to maintain a given interface configuration as determined from the density functional. For this separation of the fluctuations, density functional theory is particularly suited because the forms of the density functional which are actually available do not contain these large interface fluctuations which lead to the roughening of fluid interfaces in the absence of gravity.

The usual approach to derive an effective Hamiltonian of an interface is the expansion of a free energy into powers of curvatures of the interface with the leading terms determined by special interface configurations, i.e., spherical and cylinderical ones [10,11]. This approach yields the so-called Helfrich Hamiltonian [12,13]. Here, we derive—without using such a gradient expansion—a nonlocal and non-Gaussian expression for the effective Hamiltonian of the bending modes of a fluctuating liquid-vapor interface. Due to the long-ranged dispersion forces, nonanalytic contributions occur and therefore a gradient expansion of the Hamiltonian breaks down.

The Hamiltonian derived here improves a previous version [14] in three respects. First, we take into account a smooth variation of the intrinsic profile instead of a steplike one. Second, we incorporate the deformation of the intrinsic profile due to curvatures. Third, in analogy to the derivation of the drumhead model starting from a phenomenological Landau theory [15] we introduce normal coordinates in order to use an appropriately adapted parametrization of the density profile near the interface. These improvements put us into the position to make quantitatively reliable predictions for scattering experiments.

In Sec. II we derive the effective Hamiltonian and discuss its main features which can be inferred already within the Gaussian approximation (Sec. III). In particular we obtain an expression for the momentum-dependent surface tension $\sigma(q)$ which in the limit $q\to 0$ is consistent with the Triezenberg-Zwanzig formula [16]. In Sec. IV we summarize our results and discuss their implications for the interpretation of scattering experiments.

II. EFFECTIVE INTERFACE HAMILTONIAN

In this section we derive for arbitrary intrinsic density profiles an effective Hamiltonian for the local interface position by starting from a microscopic density functional theory for inhomogeneous fluids (Sec. II A). In Sec. II B we introduce normal coordinates in order to obtain an appropriate description of the interface configurations.

A. Density functional theory

Our analysis is based on a simple version of density functional theory for one-component fluids which consist of particles with a rotationally symmetric pair interaction potential $W(r)$. Within this approach the interaction potential $W(r)=w_s(r)+w(r)$ is split into a short-ranged repulsive part $w_s(r)$ and a long-ranged attractive part $w(r)$ [17]. The grand canonical density functional reads

$$\Omega[\rho(\mathbf{r})]=\int_V d^3r f_h(\rho(\mathbf{r}))+\mu\int_V d^3r\rho(\mathbf{r})+\int_V d^3r\rho(\mathbf{r})V(\mathbf{r})+\frac{1}{2}\int_V d^3r\int_V d^3r' w(|\mathbf{r}-\mathbf{r}'|)\rho(\mathbf{r})\rho(\mathbf{r}'), \tag{2.1}$$

where V is the volume of the sample, $\rho(\mathbf{r})$ the number density of the fluid particles at $\mathbf{r}=(x,y,z)$, and $f_h(\rho)$ is the reference free energy of a system determined by the short-ranged contribution to the interaction potential $w_s(r=|\mathbf{r}-\mathbf{r}'|)$ [17]. Considering particles which interact via dispersion forces for the attractive part of the interaction potential $w(r)$ we adopt the form [14]

$$w(r)=-\frac{w_0 r_0^6}{(r_0^2+r^2)^3}\to -Ar^{-(d+\tau)},\quad r\to\infty, \tag{2.2}$$

reflecting the correct large distance behavior $w(r)\sim r^{-6}$ for $(d,\tau)=(3,3)$ and $A=w_0r_0^6$ [18]; w_0 is the depth of $W(r)$ [18] and d denotes the spatial dimension. The length r_0 corresponds to the diameter of the particles [18] and thus serves as a lower limit for the length scale of the density fluctuations and of the capillary waves considered below. Since we are interested in length scales larger than r_0, we treat the free energy functional for the inhomogeneous density in the local approximation $f_h(\rho=\rho(\mathbf{r}))$ [17,19]. Actually $w(r)$ should be replaced by the direct correlation function $c^{(2)}(r)$ which, however, reduces to $W(r)$ and thus to $w(r)$ for large r. This replacement does not alter our main results. However, we emphasize that most of our results do not depend on the actual form of $w(r)$. This form only matters for the quantitative results presented at the end of Sec. III. For these calculations we adopt the Carnahan-Starling expression for $f_h(\rho)$ [17]:

$$f_h(\rho)=k_BT\rho\left\{\ln(\rho\lambda^3)-1+\frac{4\eta-3\eta^2}{(1-\eta)^2}\right\}, \tag{2.3}$$

where λ is the thermal de Broglie wavelength and $\eta=(\pi/6)\rho r_0^3$ the packing fraction.

Within this approach the equilibrium density profile minimizes the density functional in Eq. (2.1) and yields the grand canonical potential. The equilibrium profile depends on the temperature T, the chemical potential μ, and a possible external potential $V(\mathbf{r})$. For our purpose we consider a fluid in a gravitational field G with

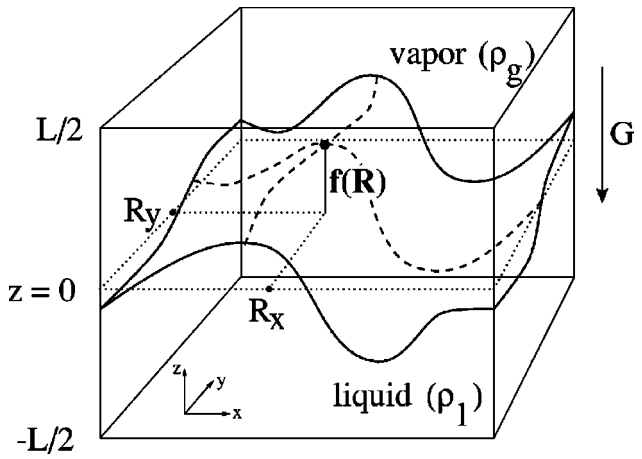

FIG. 1. Schematic picture of an interface configuration between the coexisting liquid and vapor bulk phases with number densities ρ_l and ρ_g, respectively. The interface does not contain overhangs or bubbles. Thus the local position of the liquid-vapor interface can be described by a single-valued function $f(\mathbf{R})$, where $\mathbf{R}=(R_x,R_y)$ denotes the lateral coordinates. The dashed curves indicate the intersections between the two-dimensional manifold $f(\mathbf{R})$ and the planes $x=R_x=\text{const}$ and $y=R_y=\text{const}$, respectively. Gravity $\mathbf{G}$ leads to a mean interface position at $z=0$. The volume of the sample is $V=AL$.

$$V(\mathbf{r})=mGz, \tag{2.4}$$

where m is the mass of the fluid particles. The sample volume V provides a lower bound for $V(\mathbf{r})$ such that $z=0$ corresponds to the mean interface position.

We describe the local position of the liquid-vapor interface by $z=f(\mathbf{R})$, where $\mathbf{R}=(x,y)$ with $R=|\mathbf{R}|$ is the lateral reference point in the xy plane parallel to the mean interface at $z=0$ (see Fig. 1). There are various possibilities to define the local position of such an interface from a given density distribution $\rho(\mathbf{r})$. We choose a crossing criterion, i.e., a connected isodensity contour $\rho((\mathbf{R},f(\mathbf{R})))=\rho^*$ where ρ^* is an arbitrary, fixed density. A natural choice would be the mean density $\rho^*=\overline{\rho}:=(\rho_l+\rho_g)/2$ of the bulk phases, but we do not fix this choice. Overhangs of the interface are neglected so that we can proceed analytically by treating a single-valued function $f(\mathbf{R})$. Bubbles of one phase inside the other, i.e., domains topologically separated from the interface, are assumed to give rise to a smooth intrinsic density profile $\rho_{\text{int}}(\mathbf{r};\{f(\mathbf{R})\},\rho^*)$ which depends not only on $\mathbf{r}$ but which is also a functional of the prescribed position $f(\mathbf{R})$ of the interface. We define $\rho_{\text{int}}(\mathbf{r};\{f(\mathbf{R})\},\rho^*)$ as that density profile which minimizes the grand canonical potential $\Omega[\rho(\mathbf{r})]$ under the constraint

$$\rho(\mathbf{r}=(\mathbf{R},z=f(\mathbf{R})))=\rho^*, \tag{2.5}$$

with a given fixed interface position $f(\mathbf{R})$. This minimum depends parametrically on $f(\mathbf{R})$ and ρ^* yielding the intrinsic profile $\rho_{\text{int}}(\mathbf{r};\{f(\mathbf{R}\},\rho^*)$. In this way we separate operationally in a well-defined manner the different types of density fluctuations, i.e., bulk bubbles and undulations of the interface. Of course it remains to be proved that measurable physical quantities do not depend on our choice of the definition of the interface [Eq. (2.5)]. This serves as an important check of consistency.

We use the abbreviation

$$\rho_f(\mathbf{r}):=\rho_{\text{int}}(\mathbf{r};\{f(\mathbf{R})\},\rho^*) \tag{2.6}$$

in order to keep in mind the dependence of the density profile on the chosen interface position f but without indicating the dependence on ρ^* except in cases where it is essential. In particular we define

$$\rho_0(z):=\rho_{\text{int}}(\mathbf{r};\{f(\mathbf{R})=0\},\rho^*) \tag{2.7}$$

as the intrinsic density profile of a flat interface which depends only on the distance z perpendicular to the mean interface position at $z=0$. Thus the density profile $\rho_0(z)$ is determined by the equation [see Eq. (2.1)]

$$0=\mu_h(\rho(\mathbf{r}))+\mu+mGz+\int_V d^3r'\,w(|\mathbf{r}-\mathbf{r}'|)\rho(\mathbf{r}'), \tag{2.8}$$

with $\rho_0(z=0)=\rho^*$, where we have introduced the chemical potential

$$\mu_h(\rho)=\frac{\partial f_h(\rho)}{\partial\rho} \tag{2.9}$$

of the reference system determined by the short-ranged contributions of the interactions. We would like to mention that it will turn out in the following that we do not need an equivalent *explicit* equation for the constrained density profile $\rho_f(\mathbf{r})$ for $f\neq 0$. It is important to note that as long as gravity and a finite sample volume are not important the profile $\rho_0(z,\rho^*)$ for a flat interface depends transparently on the definition of the interface, i.e., on ρ^*.

For $G=0$ and $V=\mathbb{R}^3$, Eq. (2.8) has an infinite number of solutions with the same free energy. These solutions differ by a translation in the z direction. The requirement $\rho_0(z=0)=\rho^*$ selects uniquely one solution $\rho_0(z,\rho^*)$ out of this infinite set. The solution corresponding to a different choice $\overline{\rho}^*$ instead of ρ^* is obtained from $\rho_0(z,\rho^*)$ according to $\rho_0(z,\overline{\rho}^*)=\rho_0(z+\overline{z},\rho^*)$ where $\overline{z}$ is determined implicitly by the relation $\rho_0(z=\overline{z},\rho^*)=\overline{\rho}^*$.

The effective Hamiltonian of the interface is defined as the difference

$$\mathcal{H}[f(\mathbf{R})]:=\Omega[\rho_f(\mathbf{r})]-\Omega[\rho_0(z)], \tag{2.10}$$

which describes the cost in free energy for deviations of the configuration $f(R)$ from a flat one and therefore represents the effective free energy associated with the capillary waves. It is necessary to subtract the free energy of a flat interface before an expansion in terms of the local curvature of the bent interface $f(\mathbf{R})$ can be performed. This subtraction can be accomplished explicitly by carrying out a partial integration in Eq. (2.1) for the grand canonical functional. It leads to the following expression for the effective Hamiltonian:

$$\mathcal{H}[f(\mathbf{R})]=-\int_A d^2R\int_{-\infty}^{\infty}dz\left[z\mu+\frac{mG}{2}z^2\right]\left[\frac{\partial\rho_f(\mathbf{r})}{\partial z}-\frac{\partial\rho_0(z)}{\partial z}\right]-\int_A d^2R\int_{-\infty}^{\infty}dz\left[z\mu_h(\rho_f(\mathbf{r}))\frac{\partial\rho_f(\mathbf{r})}{\partial z}-z\mu_h(\rho_0(z))\frac{\partial\rho_0(z)}{\partial z}\right]$$
$$-\frac{1}{2}\int\int_A d^2Rd^2R'\int\int_{-\infty}^{\infty}dzdz'w^{(2)}(|\mathbf{R}-\mathbf{R}'|,z-z')\left[\frac{\partial\rho_f(\mathbf{r})}{\partial z}\frac{\partial\rho_f(\mathbf{r}')}{\partial z'}-\frac{\partial\rho_0(z)}{\partial z}\frac{\partial\rho_0(z')}{\partial z'}\right]$$
$$+w^{(0)}\overline{\rho}\int_A d^2R\int_{-\infty}^{\infty}dzz\left(\frac{\partial\rho_f(\mathbf{r})}{\partial z}-\frac{\partial\rho_0(z)}{\partial z}\right). \tag{2.11}$$

The projected area A of the interface $f(\mathbf{R})$ onto the plane $z=0$ is the lateral cross section of the container volume $V=AL$. The constant $w^{(0)}$ is the integrated strength of the attractive part of the interaction potential,

$$w^{(0)}=-\int_{\mathbb{R}^3}d^3rw(|\mathbf{r}|)=-2\int_{\mathbb{R}^2}d^2Rw^{(1)}(\mathbf{R},z=\infty)>0 \tag{2.12}$$

[$w^{(0)}=\pi^2w_0r_0^3/4$ for Eq. (2.2)], and the functions $w^{(1)}$ and $w^{(2)}$ are defined as

$$w^{(1)}(|\mathbf{R}|,z)=\int_0^z dz'w(\sqrt{\mathbf{R}^2+z'^2}) \tag{2.13}$$

and

$$w^{(2)}(|\mathbf{R}|,z)=\int_0^z dz'\int_0^{z'}dz''w(\sqrt{\mathbf{R}^2+z''^2}), \tag{2.14}$$

respectively. Due to $w^{(1)}(|\mathbf{R}|,z=0)=0$ and the rotational symmetry of $w(r)$, the function $w^{(1)}(|\mathbf{R}|,z)=-w^{(1)}(|\mathbf{R}|,-z)$ is antisymmetric and $w^{(2)}(|\mathbf{R}|,z)=w^{(2)}(|\mathbf{R}|,-z)$ is symmetric.

The validity of Eq. (2.11) is based on two conditions. First, we have assumed that at the top ($z=+L/2$) and at the bottom ($z=-L/2$) of the containers $\rho_f(\mathbf{r})$ and $\rho_0(z)$ have the same values so that the corresponding boundary terms in the partial integration drop out. Since gravity prevents large excursions of $f(\mathbf{R})$ which come close to $z=\pm L/2$, this assumption seems to be justified. Only the last contribution in Eq. (2.11) stems from boundary terms of the partial integration which appear in the course of the derivation of Eq. (2.11) as follows:

$$\int_{\mathbb{R}^2}d^2Rw^{(1)}(|\mathbf{R}-\mathbf{R}'|,z-z')\rho_0(z)|_{z\to-\infty}^{z\to\infty}$$
$$=-w^{(0)}\frac{\rho_l+\rho_g}{2}=-w^{(0)}\overline{\rho}. \tag{2.15}$$

We note that although in Eq. (2.15) we have taken the limit $A\to\mathbb{R}^2$, the last term in Eq. (2.11) still contains a finite area A of integration. Rather generally for large A the effective Hamiltonian scales with A. Accordingly the line contributions due to the difference between $\rho_f(\mathbf{r})$ and $\rho_0(z)$ at the lateral boundaries drop out in the thermodynamic limit $A\to\infty$ envisaged in Eq. (2.11).

The second condition entering Eq. (2.11) is that the limits $\pm L/2$ of the z integrations can be shifted to infinity. In the absence of gravity $\rho_0(z)$ and $\rho_f(\mathbf{r})$ approach the bulk values ρ_g and ρ_l for $|z|\to\infty$ according to vdW tails $\sim z^{-3}$ [20] which render the integrals in Eq. (2.11) finite. Furthermore, we consider only sample volumes which are sufficiently small so that the influence of gravity on the shape of the profiles $\rho_f(\mathbf{r})$ and $\rho_0(z)$ can be neglected and the above convergence arguments for the integrals remain valid. Therefore in the following we take $\rho_0(z)$ as the solution of Eq. (2.8) with $G=0$ and the boundary conditions $\rho_0(z\to\infty)=\rho_g$ and $\rho_0(z\to-\infty)=\rho_l$ where ρ_g and ρ_l are the coexisting bulk densities in the absence of gravity.

B. Normal coordinates

In the next step we derive a formula for the intrinsic density profile $\rho_f(\mathbf{r})$ which enables us to express the effective interface Hamiltonian given by Eq. (2.11) *explicitly* in terms

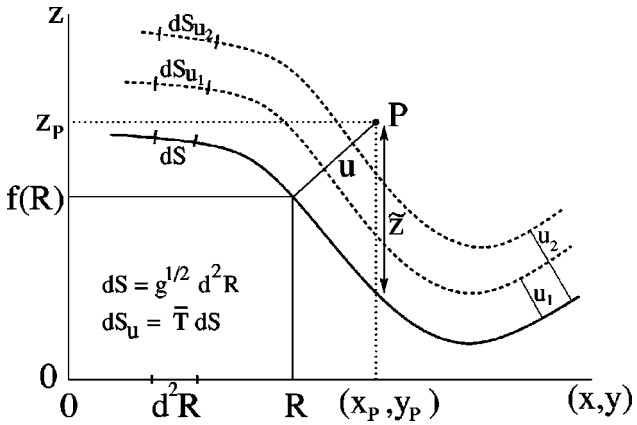

FIG. 2. Intersection of the manifold $f(\mathbf{R})$ with a plane whose normal lies in the xy plane. The normal coordinates $(\mathbf{R},u)$ of a point $P=(x_P,y_P,z_P)=(\mathbf{R}_P,z_P)$ are defined by the minimal distance u to the interface $f(\mathbf{R})$. We emphasize that the lateral coordinates x_P and y_P of P are not identical to the lateral interface position $\mathbf{R}$ of that point of the manifold which has the minimal distance to P. The dashed lines are the corresponding intersections with parallel surfaces distances u_1 and u_2 apart from $f(\mathbf{R})$. The normalized Jacobian $\overline{T}$ takes into account the variation of the area element $dS_u=\overline{T}dS$ between parallel surfaces given by $\overline{T}:=|T|/\sqrt{g}=[\partial(x,y,z)/\partial(R_x,R_y,u)]/\sqrt{g}=(1+\delta\overline{T})$, where $g=1+[\nabla f(\mathbf{R})]^2$ is the metric of the interface $f(\mathbf{R})$. If the point P is far apart from $f(\mathbf{R})$ the minimal distance u and $\mathbf{R}$ reduce to $\tilde{z}=z_P-f(\mathbf{R}_P)$ and $\mathbf{R}_P$, respectively.

of $f(\mathbf{R})$. The physical picture is that the minimization procedure based on Eq. (2.5) leads to an intrinsic density profile $\rho_f(\mathbf{r})$ of three variables x,y, and z which is locally similar to the intrinsic profile of the flat configuration provided the density variation is measured along the local normal of the manifold $f(\mathbf{R})$. More generally we approximate the actual density profile $\rho_f(\mathbf{r})$ depending on $\mathbf{r}=(\mathbf{R},z)$ by a function $\hat{\rho}_f(u)$ which for a fixed configuration $f(\mathbf{R})$ depends only on a *single* variable u given by the minimal distance $u_f(\mathbf{r}) := u(\mathbf{r};\{f(\mathbf{R})\})$ of the point $\mathbf{r}$ from the interface $f(\mathbf{R})$, i.e.,

$$\rho_f(\mathbf{r}) \simeq \hat{\rho}_f(u=u_f(\mathbf{r})) = \hat{\rho}(u_f(\mathbf{r});\{f(\mathbf{R})\}). \tag{2.16}$$

We note that not only the variable u but also the form of the function $\hat{\rho}_f(u)$ depends on the shape of the manifold $f(\mathbf{R})$ as indicated by the index f (see Fig. 2). For large distances from the interface the variable $u_f(\mathbf{r})$ reduces to the vertical distance $\tilde{z}=z-f(\mathbf{R})$ whereas for small $\tilde{z}$ the coordinate u is normal to the interface and thus is the distance perpendicular to the interface $f(\mathbf{R})$. In accordance with the problem under consideration the manifold $f(\mathbf{R})$ is not closed but asymptotically flat.

In order to proceed one needs to know [see Eq. (2.16)] the explicit dependence of u_f on $f(\mathbf{R})$ [see Eq. (2.21)] as well as the explicit dependence of $\hat{\rho}_f(u)$ on $f(\mathbf{R})$. With regard to the latter dependence we expand the intrinsic density profile into powers of curvatures of the interface:

$$\begin{aligned}\hat{\rho}_{f(\mathbf{R})}(u) &= \rho_0(u) + 2H\rho_H(u) + K\rho_K(u) + (2H)^2\rho_{H^2}(u) + \cdots \\ &= \rho_0(u) + \delta\rho_{f(\mathbf{R})}(u).\end{aligned} \tag{2.17}$$

With the abbreviations $f_j := \partial f(\mathbf{R})/\partial j$, $j=x,y$, K denotes the Gaussian curvature,

$$K = \frac{1}{2g^2}[f_{xx}(\mathbf{R})f_{yy}(\mathbf{R}) - f_{yx}(\mathbf{R})f_{xy}(\mathbf{R})], \tag{2.18}$$

H the mean curvature,

$$H = \frac{f_{xx}(\mathbf{R})\{1+[f_y(\mathbf{R})]^2\} + f_{yy}(\mathbf{R})\{1+[f_x(\mathbf{R})]^2\} - 2f_x(\mathbf{R})f_y(\mathbf{R})f_{xy}(\mathbf{R})}{2g^{3/2}} = \frac{1}{2}\Delta f(\mathbf{R}) + O\left(\left(\frac{\partial^k f}{\partial_j^k}\right)^2\right), \quad k \geqslant 1, \tag{2.19}$$

and g the metric

$$g = 1 + [\nabla f(\mathbf{R})]^2 \tag{2.20}$$

of the interface $f(\mathbf{R})$.

In principle, the distortion $\delta\rho_{f(\mathbf{R})}(u)$ of the density profile due to the bending of the interface $f(\mathbf{R})$ can be inferred from considering spherical and cylindrical interfaces $f(\mathbf{R})$ (see, e.g., Ref. [10]). However, whereas it is known that the profile $\rho_0(u)$ is positive for all values of u and interpolates smoothly between the bulk densities ρ_l for $u\to-\infty$ and ρ_g for $u\to\infty$, there are no explicit results for the profiles $\rho_H(u)$, $\rho_K(u)$, and $\rho_{H^2}(u)$. We expect that the correction term $\rho_H(u)$ due to the mean curvature H of the interface at $\mathbf{R}$ is also positive. This means that there is an increase of the density $\hat{\rho}_f(u)$ compared with $\rho_0(u)$ if the interface is bent locally towards the vapor phase, i.e., for $H>0$, and a decrease for $H<0$. The reasoning for this sign is that for a given distance u below (above) the interface $f(\mathbf{R})$ the corresponding point appears to be effectively deeper (less deep) in the liquid (vapor) phase due to $H(\mathbf{R})>0$ as compared with ρ_0 for a flat interface evaluated at the same u. In the following we make no further assumptions about the functional form of the correction terms $\rho_\lambda(u)$, $\lambda=H,K,H^2$. But it is important to note that in contrast to $\rho_0(z,\rho^*)$ the distortions $\rho_\lambda(u,\rho^*)$ depend less transparently on the choice of the crossing criterion ρ^*.

According to the concept introduced at the beginning of this subsection the profiles $\rho_0(u)$ and $\rho_\lambda(u)$ are evaluated at the minimal distance u as determined by the normal coordinates (R_x,R_y,u). They are related to the Cartesian coordinates (x,y,z) and the representation $f(\mathbf{R})$ of the interface according to (see, e.g., Ref. [15] and Fig. 2)

$$\begin{pmatrix} x \\ y \\ z \end{pmatrix} = \begin{pmatrix} R_x \\ R_y \\ f(\mathbf{R}) \end{pmatrix} + u\mathbf{n}(\mathbf{R}). \tag{2.21}$$

The normal is given by the vector $\mathbf{n}(\mathbf{R})=(-\nabla f(\mathbf{R}),1)/\sqrt{g}$ and the Jacobian $|T|$ of this transformation is

$$|T| = \frac{\partial(x,y,z)}{\partial(R_x,R_y,u)} =: \sqrt{g}\overline{T} =: \sqrt{g}(1+\delta\overline{T}), \tag{2.22}$$

with [based on Eq. (2.21)]

$$\overline{T} = (1+u\partial_{R_x}n_x)(1+u\partial_{R_y}n_y) = |1-2uH+u^2K|. \tag{2.23}$$

Whereas this transformation in Eq. (2.21) is correct for small values of u, it does not hold for large values of u due to singularities in the transformation given by Eq. (2.21). These singularities are caused by the intersection of normal vectors $u\mathbf{n}(\mathbf{R}_1)$ and $u\mathbf{n}(\mathbf{R}_2)$ at different interface positions $\mathbf{R}_1$ and $\mathbf{R}_2$. Thus for a given point $\mathbf{r}=(x,y,z)$ there can be more than one corresponding tupel (R_x,R_y,u). The approximate character of this transformation shows up, *inter alia*, at large distances u from the interface for which the variable u reduces to $\tilde{z}=z-f(\mathbf{R})$ and the normal vector $\mathbf{n}(\mathbf{R})$ becomes vertical. In this limit the foot point $(\mathbf{R},f(\mathbf{R}))$ of the normal is given by the point nearest to (x,y) where the interface $f(\mathbf{R})$ has a maximum, i.e., where $f(\mathbf{R})$ is horizontal with $\nabla f(\mathbf{R})=0$. Therefore one has $g(\mathbf{R}(u\to\infty))=1$. Thus the Jacobian

$|T|$ of this latter transformation is equal to 1 in contrast to the large-u behavior given by Eqs. (2.22) and (2.23). However, since the integrands of the Hamiltonian in Eq. (2.11) are proportional to the first derivatives of the profiles $\rho_f(\mathbf{r})$ and $\rho_0(z)$, they are peaked around $z=f(\mathbf{R})$ or $z=0$, respectively. Thus the main contributions to these integrals stem from small values of u. Therefore the aforementioned deficiency of the transformation for large values of u is effectively suppressed. A more detailed account of this mechanism is given below.

C. Explicit form of the effective interface Hamiltonian

According to Secs. II A and II B the dependence of the Hamiltonian $\mathcal{H}$ in Eq. (2.11) on the interface position $f(\mathbf{R})$ stems from two sources. First, one obtains terms which depend on $f(\mathbf{R})-f(\mathbf{R}')$ due to the nonlocality of the potential $w^{(2)}(|\mathbf{R}-\mathbf{R}'|,z-z')$ as a function of z and z'. Second, there appear terms involving $\nabla f(\mathbf{R})$ and higher derivatives of $f(\mathbf{R})$ due to the transformation in Eq. (2.21) and, in particular, due to the metric g and the Jacobian $|T|$. We keep the full dependence on $f(\mathbf{R})-f(\mathbf{R}')$ in the first type of terms but in accordance with Eqs. (2.16) and (2.17) we expand $\rho_f(\mathbf{r})$, which enters into Eq. (2.11), into powers of first derivatives and of curvatures, i.e., higher derivatives of $f(\mathbf{R})$, keeping terms $(\partial^k f/\partial j^k)^l$ with $l,k\leqslant 2$.

Accordingly in the thermodynamic limit for large A the Hamiltonian $\mathcal{H}$ consists of three contributions, one due to gravity (G) as well as local (l) and nonlocal (nl) terms:

$$\mathcal{H}[f(\mathbf{R})]=\mathcal{H}_G[f(\mathbf{R})]+\mathcal{H}_l[f(\mathbf{R})]+\mathcal{H}_{nl}[f(\mathbf{R})]. \tag{2.24}$$

In the field of gravity the displacement of the interface position relative to the reference plane $z=0$ leads to the following energy contributions:

$$\mathcal{H}_G[f(\mathbf{R})]=\frac{1}{2}mG\Delta\rho\int_A d^2R\{[f(\mathbf{R})]^2+\delta^{(T)}[f(\mathbf{R})] +2f(\mathbf{R})\,\delta^{(\rho)}[f(\mathbf{R})]\}, \tag{2.25}$$

with the moment

$$\delta^{(T)}[f(\mathbf{R})]=\frac{1}{\Delta\rho}\int_{-\infty}^{\infty}du\,\delta\overline{T}u^2\frac{\partial\rho_0(u)}{\partial u} \tag{2.26}$$

due to the change of the area $|T|$ of the parallel surface and thus of the mass distribution. The second gravity contribution [see Eq. (2.17)]

$$\delta^{(\rho)}[f(\mathbf{R})]=\frac{1}{\Delta\rho}\int_{-\infty}^{\infty}du\,\delta\rho_f(u)=:2H\delta_H+K\delta_K+(2H)^2\delta_{H^2} +\cdots \tag{2.27}$$

with

$$\delta_\lambda=\frac{1}{\Delta\rho}\int_{-\infty}^{\infty}du\,\rho_\lambda(u),\quad \lambda=H,H^2,K, \tag{2.28}$$

stems from a shift of mass across the interface due to the distortion $\delta\rho_f(u)$ of the bent interface profile.

The second term in Eq. (2.24) contains contributions proportional to the mean curvature H, to the Gaussian curvature K, and to the square of the mean curvature of the interface and thus collects the local bending energies:

$$\mathcal{H}_l[f(\mathbf{R})]=\int_A d^2R\{\kappa^{(T)}[f(\mathbf{R})]+\kappa^{(\rho)}[f(\mathbf{R})]\}, \tag{2.29}$$

with

$$\begin{aligned}\kappa^{(T)}[f(\mathbf{R})]&=-\int_{-\infty}^{\infty}du[\mu_h(\rho_0(u))\\ &\quad+\mu-w^{(0)}\overline{\rho}+mGu]u\,\delta\overline{T}\frac{\partial\rho_0(u)}{\partial u}\\ &=\int\int_{-\infty}^{\infty}du\,du'\int_{\mathbb{R}^2}d^2Rw^{(1)}(R,u-u')\\ &\quad\times u\,\delta\overline{T}\frac{\partial\rho_0(u)}{\partial u}\,\frac{\partial\rho_0(u')}{\partial u'}\end{aligned} \tag{2.30}$$

and

$$\begin{aligned}\kappa^{(\rho)}[f(\mathbf{R})]&=-\int_{-\infty}^{\infty}du\left(\frac{\partial^2 f_h(\rho_0)}{\partial\rho_0^2}u\,\delta\rho_f(u)\frac{\partial\delta\rho_f(u)}{\partial u}\right.\\ &\quad\left.+\frac{1}{2}\frac{\partial^3 f_h(\rho_0)}{\partial\rho_0^3}u[\delta\rho_f(u)]^2\frac{\partial\rho_0(u)}{\partial u}\right)\\ &=\frac{1}{2}\int_{-\infty}^{\infty}du\frac{\partial^2 f_h(\rho_0)}{\partial\rho_0^2}[\delta\rho_f(u)]^2\\ &=\frac{1}{2}\kappa(2H)^2+\cdots,\end{aligned} \tag{2.31}$$

with

$$\kappa=\int_{-\infty}^{\infty}du\left.\frac{\partial^2 f_h(\rho)}{\partial\rho^2}\right|_{\rho=\rho_0(u)}[\rho_H(u)]^2>0. \tag{2.32}$$

The second equation in Eq. (2.30) follows from the first one by using Eq. (2.8). The relations in Eq. (2.31) can be obtained by partial integration. The occurrence of these local bending rigidities reflects the smoothness of the intrinsic density profile. As one can see from Eqs. (2.30)–(2.32) they vanish within the sharp-kink approximation $\rho_0^{(sk)}(u)=\rho_l-\Delta\rho\Theta(u)$ with the Heaviside function $\Theta(u)$ used in Ref. [14] which leads to $\partial\rho_0^{(sk)}(u)/\partial u=-\Delta\rho\,\delta(u)$. As one can see from the second equation in Eq. (2.31) the bending rigidity κ is always positive, ensuring the stability of the interface against perturbations with large wave vectors. This positive bending rigidity is linked to the presence of the distortion $\rho_H(u)$ of the flat intrinsic density profile induced by the curvature of the interface [see Eq. (2.17)]. This demonstrates the importance of keeping track of the change of the local density near the interface due to its curvature in order to obtain a reliable expression of the cost in free energy of bent interfaces.

Equations (2.26) and (2.30) contain moments of the derivative of the flat intrinsic profile multiplied by the deviation $\delta\overline{T}=\overline{T}-1$ of the Jacobian divided by $\sqrt{g}$ from its value for a flat interface [see Eq. (2.22)]. For small values of u, for which Eq. (2.23) is valid, $\delta\overline{T}(u)=-2uH+u^2K$ consists of a term linear in u and of a term quadratic in u. On the other hand, as discussed in the paragraph following Eq. (2.23), for large u one has $|T|=1$ and $\sqrt{g(\mathbf{R}(u\to\infty))}=1$ so that $\delta\overline{T}(u\to\infty)=0$, a value not captured by Eq. (2.23). This leveling off of $\delta\overline{T}(u)$ for large u ensures the convergence of the integrals in Eqs. (2.26) and (2.30) even in the presence of dispersion forces which cause an algebraic decay of $\partial\rho_0(u)/\partial u\sim|u|^{-4}$ for $|u|\to\infty$ [20]. Regrettably there is no explicit formula available which covers the full dependence of $\delta\overline{T}(u)$ for all values of u. However, since $\partial\rho_0(u)/\partial u$ is peaked around $u=0$, the main contributions to $\delta^{(T)}[f(\mathbf{R})]$ and $\kappa^{(T)}[f(\mathbf{R})]$ stem from small values of u for which the explicit form of $\delta\overline{T}(u)$ is given by Eq. (2.23). The width of this relevant region of values for u is set by the bulk correlation length ξ [20] so that we obtain the following explicit albeit approximate expressions for $\delta^{(T)}$ and $\kappa^{(T)}$:

$$\delta^{(T)}[f(\mathbf{R})]\simeq-2H\delta_3+K\delta_4, \tag{2.33}$$

with

$$\delta_n=\frac{1}{\Delta\rho}\int_{-\xi}^{\xi}du\,u^n\frac{\partial\rho_0(u)}{\partial u},\quad \Delta\rho=\rho_l-\rho_g, \tag{2.34}$$

and

$$\kappa^{(T)}[f(\mathbf{R})]\simeq-2H\overline{\kappa_2}+K\overline{\kappa_3}+\cdots, \tag{2.35}$$

with

$$\overline{\kappa_n}=\int\int_{-\xi}^{\xi}du\,du'\int_{\mathbb{R}^2}d^2R\,w^{(1)}(R,u-u')\times u^n\frac{\partial\rho_0(u)}{\partial u}\frac{\partial\rho_0(u')}{\partial u'}. \tag{2.36}$$

For asymptotically flat interfaces as considered here $\int_A d^2RK=0$ so that the terms $K\delta_4$ and $K\overline{\kappa_3}$ have not to be considered in the following.

The third term in the Hamiltonian in Eq. (2.24) takes into account the nonlocal contributions mentioned above:

$$\begin{aligned}\mathcal{H}_{nl}[f(\mathbf{R})]=&\int\int_A d^2R\,d^2R'\Big[h(\delta\mathbf{R},\delta f)+\frac{1}{2}[\nabla f(\mathbf{R})]^2\sigma(\delta\mathbf{R},\delta f)\Big]\\&+\int\int_A d^2R\,d^2R'[2H\kappa^{(H)}(\delta\mathbf{R},\delta f)+(2H)^2\kappa^{(H^2)}(\delta\mathbf{R},\delta f)+K\kappa^{(K)}(\delta\mathbf{R},\delta f)]\\&-\frac{1}{2}\int\int_A d^2R\,d^2R'\Delta f(\mathbf{R})\Delta f(\mathbf{R}')\kappa^{(HH)}(\delta\mathbf{R},\delta f)+\cdots.\end{aligned} \tag{2.37}$$

Here, we have introduced the abbreviations $\delta f:=\delta f(\mathbf{R},\mathbf{R}')=f(\mathbf{R})-f(\mathbf{R}')$ and $\delta\mathbf{R}:=\mathbf{R}-\mathbf{R}'$. All derivatives, if not indicated otherwise, are evaluated at $\mathbf{R}$. With the notations $\delta u:=u-u'$ and $\lambda=H,H^2,K$ the integrands in Eq. (2.37) are given by

$$\begin{aligned}h(\delta\mathbf{R},\delta f)=&-\frac{1}{2}\int\int_{-\infty}^{\infty}du\,du'\frac{\partial\rho_0(u)}{\partial u}\frac{\partial\rho_0(u')}{\partial u'}\\&\times[w^{(2)}(\delta\mathbf{R},\delta u+\delta f)-w^{(2)}(\delta\mathbf{R},\delta u)\\&-w^{(1)}(\delta\mathbf{R},\delta u)\,\delta f],\end{aligned} \tag{2.38}$$

$$\begin{aligned}\sigma(\delta\mathbf{R},\delta f)=&-\int\int_{-\infty}^{\infty}du\,du'[w^{(1)}(\delta\mathbf{R},\delta u+\delta f)\\&-w^{(1)}(\delta\mathbf{R},\delta u)]u\frac{\partial\rho_0(u)}{\partial u}\frac{\partial\rho_0(u')}{\partial u'},\end{aligned} \tag{2.39}$$

$$\begin{aligned}\kappa^{(\lambda)}(\delta\mathbf{R},\delta f)=&\int\int_{-\infty}^{\infty}du\,du'[w^{(1)}(\delta\mathbf{R},\delta u+\delta f)\\&-w^{(1)}(\delta\mathbf{R},\delta u)]\rho_\lambda(u)\frac{\partial\rho_0(u')}{\partial u'},\end{aligned} \tag{2.40}$$

and

$$\begin{aligned}\kappa^{(HH)}(\delta\mathbf{R},\delta f)=&\int\int_{-\infty}^{\infty}du\,du'\,w^{(2)}(\delta\mathbf{R},\delta u+\delta f)\\&\times\frac{\partial\rho_H(u)}{\partial u}\frac{\partial\rho_H(u')}{\partial u'}\\=&-\int\int_{-\infty}^{\infty}du\,du'\,w[\sqrt{(\delta\mathbf{R})^2+(\delta u+\delta f)^2}]\\&\times\rho_H(u)\rho_H(u').\end{aligned} \tag{2.41}$$

These terms take into account the nonlocal effects caused by the interaction potential $w(r)$. We emphasize that Eqs. (2.37)–(2.41) capture the *full* dependence of the interface free energy $\mathcal{H}$ on the difference $\delta f=f(\mathbf{R})-f(\mathbf{R}')$ for small values of u so that the resulting Hamiltonian is non-Gaussian and nonlocal.

The derivation of Eq. (2.24) uses explicitly the equilibrium condition in Eq. (2.8) for the flat intrinsic profile which leads to the cancellation of all terms proportional to $f(\mathbf{R})$ in the Hamiltonian in Eq. (2.24). This is necessary for obtaining an equilibrium mean interface position at $z=0$, i.e., $\langle f(\mathbf{R})\rangle=0$. Here, $\langle\cdot\rangle$ denotes the thermal average with $\exp(-\beta\mathcal{H})$ as the statistical weight.

It is pleasing to see that the general form of the nonlocal contribution in Eq. (2.37) is also given by an expansion in terms of local derivatives of the interface position $f(\mathbf{R})$. But in contrast to the local contribution in Eq. (2.29), the expansion coefficients depend nonlocally on the interface position $f(\mathbf{R})$ due to the nonzero range of the pair potential $w(r)$ in the density functional in Eq. (2.1).

In the special case of the sharp-kink approximation $\rho_0^{(sk)}(u)=\rho_g\Theta(u)+\rho_l\Theta(-u)$ for the intrinsic density profile the Hamiltonian in Eq. (2.24) reduces to

$$\mathcal{H}^{(sk)}[f(\mathbf{R})]=\frac{1}{2}mG\Delta\rho\int_A d^2R[f(\mathbf{R})]^2 - \frac{\Delta\rho^2}{2}\int\int_A d^2R\,d^2R'[w^{(2)}(\delta\mathbf{R},\delta f) - w^{(2)}(\delta\mathbf{R},0)-w^{(1)}(\delta\mathbf{R},0)\delta f], \quad (2.42)$$

which coincides with the expression derived in Ref. [14]. *Inter alia*, as mentioned above, within this sharp-kink approximation the contributions proportional to curvatures of the interface vanish. Thus the sharp-kink approximation is not applicable for the description of bendings of the interface with short wavelengths.

Since the equilibrium profile $\rho_0(u)$ is independent of the choice of the crossing criterion ρ^*, the functions $h(\delta\mathbf{R},\delta f)$ and $\sigma(\delta\mathbf{R},\delta f)$ and therefore the surface tension σ_0 [see Eq. (3.12)] are independent of it, too. But the dependence of the distortion $\delta\rho(u)$, i.e., of $\rho_\lambda(u,\rho^*)$, on the crossing criterion ρ^* induces such a dependence of the bending rigidities κ, $\kappa^{(\lambda)}(\delta\mathbf{R},\delta f)$, and $\kappa^{(HH)}(\delta\mathbf{R},\delta f)$. So different choices of ρ^* result in different functions and the rigidities must be regarded as being specific to the chosen isodensity contour as interface location. However, as mentioned already in Ref. [21] this dependence is not a defect of the present formalism. Instead it remains to be proved within our approach that for measurable quantities such as correlation functions this dependence on ρ^* drops out. Moreover, as described in Ref. [22] the dependence on ρ^* can be exploited in order to construct the lateral structure factor for normal positions $z_1,z_2\neq 0$.

III. GAUSSIAN THEORY

A. General expressions

One gains important insight into the structure of the Hamiltonian in Eq. (2.24) by truncating all contributions nonlinear in $f(\mathbf{R})$: $\mathcal{H}[f]=\mathcal{H}^{(G)}[f]+\mathcal{O}(f^3)$. In view of calculating later on thermal averages with the statistical weight $\exp(-\beta\mathcal{H}[f])$ we call this a Gaussian approximation within which we obtain

$$\mathcal{H}^{(G)}[f(\mathbf{R})]=\frac{1}{2}mG\Delta\rho\int_A d^2R\{f(\mathbf{R})^2-2\delta_H[\nabla f(\mathbf{R})]^2\}+\frac{1}{2}\kappa\int_A d^2R[\Delta f(\mathbf{R})]^2 + \int\int_A d^2R\,d^2R'\left[h_0(\delta\mathbf{R})(\delta f)^2+\kappa_0^{(H)}(\delta\mathbf{R})\Delta f(\mathbf{R})\delta f-\frac{1}{2}\kappa_0^{(HH)}(\delta\mathbf{R})\Delta f(\mathbf{R})\Delta f(\mathbf{R}')\right], \quad (3.1)$$

with $\kappa>0$ given by Eq. (2.32) and with the positive definite functions

$$h_0(\delta\mathbf{R})=-\frac{1}{4}\int\int_{-\infty}^{\infty}du\,du'\,w[\sqrt{(\delta\mathbf{R})^2+(\delta u)^2}]\times\frac{\partial\rho_0(u)}{\partial u}\frac{\partial\rho_0(u')}{\partial u'} \quad >0, \quad (3.2)$$

$$\kappa_0^{(H)}(\delta\mathbf{R})=\int\int_{-\infty}^{\infty}du\,du'\,w[\sqrt{(\delta\mathbf{R})^2+(\delta u)^2}]\times\rho_H(u)\frac{\partial\rho_0(u')}{\partial u'} \quad >0, \quad (3.3)$$

and

$$\kappa_0^{(HH)}(\delta\mathbf{R})=-\int\int_{-\infty}^{\infty}du\,du'\,w[\sqrt{(\delta\mathbf{R})^2+(\delta u)^2}]\times\rho_H(u)\rho_H(u') \quad >0. \quad (3.4)$$

The local energy term $-2H\overline{\kappa}_2$ [Eq. (2.35)] and the gravity terms $-2H\delta_3$ [Eq. (2.33)] and $2H\delta_H$ [Eq. (2.27)] proportional to the mean curvature $H(\mathbf{R})\sim\Delta f(\mathbf{R})$ can be integrated, yielding boundary terms which vanish in the thermodynamic limit $A\to\infty$, because the interface is asymptotically flat. Therefore, they are omitted from Eq. (3.1). [The contributions $\sim K$ are zero as noted after Eq. (2.36)]. As already indicated at the end of Sec. II the energy term $h_0(\delta\mathbf{R})$ does not depend on the definition of the interface position. According to the paragraph following Eq. (2.9) the various possible definitions of the interface position can be mapped onto each other by suitable shifts of the argument u of the intrinsic interface profile $\rho_0(u)$. Since the integrand in Eq. (3.2) depends only on $\delta u=u-u'$, such shifts do not alter the value of $h_0(\delta\mathbf{R})$ because they can be compensated by corresponding shifts of the integration variables u and u'. In contrast, the coefficients $\kappa_0^{(H)}(\delta\mathbf{R},\rho^*)$ and $\kappa_0^{(HH)}(\delta\mathbf{R},\rho^*)$ depend on ρ^* through $\rho_H(u,\rho^*)$ describing the distortion of the intrinsic profile.

It is transparent to study $\mathcal{H}^{(G)}$ in Fourier space in which the bending modes decouple. To this end we introduce the Fourier transformed functions

$$\tilde{f}(\mathbf{q})=\int_{\mathbb{R}^2}d^2R\,e^{-i\mathbf{q}\cdot\mathbf{R}}f(\mathbf{R}), \quad f(\mathbf{R})=\int_{\mathbb{R}^2}\frac{d^2q}{(2\pi)^2}e^{i\mathbf{q}\cdot\mathbf{R}}\tilde{f}(\mathbf{q}), \quad (3.5)$$

$$\tilde{w}(q,u)=\int_{\mathbb{R}^2}d^2R\,e^{-i\mathbf{q}\cdot\mathbf{R}}w(\sqrt{\mathbf{R}^2+u^2}) =2\pi\int_0^\infty dR\,RJ_0(qR)w(\sqrt{R^2+u^2}), \quad (3.6)$$

with the Bessel function $J_0(x)$,

$$\tilde{h}_0(\mathbf{q}) = \int_{\mathbb{R}^2} d^2R e^{-i\mathbf{q}\cdot\delta\mathbf{R}} h_0(\delta\mathbf{R}) = -\frac{1}{4}\int\int_{-\infty}^{\infty} du\,du'\,\tilde{w}(\mathbf{q},\delta u)\frac{\partial\rho_0(u)}{\partial u}\frac{\partial\rho_0(u')}{\partial u'}, \tag{3.7}$$

$$\tilde{\kappa}_0^{(H)}(\mathbf{q}) = \int_{\mathbb{R}^2} d^2R e^{-i\mathbf{q}\cdot\delta\mathbf{R}} \kappa_0^{(H)}(\delta\mathbf{R}) = \int\int_{-\infty}^{\infty} du\,du'\,\tilde{w}(\mathbf{q},\delta u)\rho_H(u)\frac{\partial\rho_0(u')}{\partial u'}, \tag{3.8}$$

and

$$\tilde{\kappa}_0^{(HH)}(\mathbf{q}) = \int_{\mathbb{R}^2} d^2R e^{-i\mathbf{q}\cdot\delta\mathbf{R}} \kappa_0^{(HH)}(\delta\mathbf{R}) = -\int\int_{-\infty}^{\infty} du\,du'\,\tilde{w}(\mathbf{q},\delta u)\rho_H(u)\rho_H(u'). \tag{3.9}$$

In terms of these functions the Hamiltonian $\mathcal{H}^{(G)}$ reads

$$\mathcal{H}^{(G)}[\tilde{f}(\mathbf{q})] = \int_{\mathbb{R}^2}\frac{d^2q}{(2\pi)^2}\frac{1}{2}|\tilde{f}(\mathbf{q})|^2[mG\Delta\rho(1-2\delta_H q^2) + \sigma_0(q)q^2], \tag{3.10}$$

with the momentum-dependent surface tension

$$\sigma_0(q) = 4\frac{\tilde{h}_0(0)-\tilde{h}_0(q)}{q^2} + 2[\tilde{\kappa}_0^{(H)}(q)-\tilde{\kappa}_0^{(H)}(0)] + [\kappa-\tilde{\kappa}_0^{(HH)}(q)]q^2 + \mathcal{O}(q^4). \tag{3.11}$$

The index 0 indicates that these expressions refer to the Gaussian approximation. Equations (3.10) and (3.11) describe the cost in free energy for bending an interface with wave vector $\mathbf{q}$ in terms of the microscopic interaction potential $w(r)$ [Eq. (2.2)] [or the direct correlation function $c^{(2)}(r)$], the intrinsic density profile $\rho_0(u)$ [Eq. (2.8)] of a flat interface, and its distortion $\rho_H(u)$ [Eq. (2.17)] due to the mean curvature H of $f(\mathbf{R})$.

Since we have truncated higher derivatives of $f(\mathbf{R})$, the expression for $\sigma_0(q)$ in Eq. (3.11) is valid up to, but not including, terms of the order of q^4. This implies that the effective interface Hamiltonian $\mathcal{H}^{(G)}$ in Eq. (3.10) captures, within the Gaussian approximation, all contributions up to, but not including, terms proportional to q^6.

B. General properties

If the interparticle potential decays sufficiently rapidly, i.e., $w(r\to\infty) = -Ar^{-(d+\tau)}$ with $\tau>1$, which covers the physically relevant case of fluids in spatial dimension $d=3$ governed by dispersion forces with $\tau=3$, the momentum-dependent surface tension $\sigma_0(q)$ attains a finite positive value for $q\to 0$:

$$\sigma_0 := \sigma_0(q=0) = \frac{1}{2}\int\int_{-\infty}^{\infty} du\,du'\,\tilde{w}''(0,u-u')\times\frac{\partial\rho_0(u)}{\partial u}\frac{\partial\rho_0(u')}{\partial u'} > 0, \tag{3.12}$$

where

$$\tilde{w}''(0,u) = \left.\frac{\partial^2\tilde{w}(q,u)}{\partial q^2}\right|_{q=0} = -\int_0^{\infty} d^{d-1}R R^2 w(\sqrt{R^2+u^2}) > 0 = -\pi\int_0^{\infty} dR R^3 w(\sqrt{R^2+u^2}), \quad d=3. \tag{3.13}$$

Due to the rotational invariance of $w(r)$, one has $\tilde{w}'(0,u) = \partial\tilde{w}(q,u)/\partial q|_{q=0} = 0$.

Since $w(r)$ is smooth for $r\to 0$ and vanishes for $r\to\infty$, one has $\lim_{q\to\infty}\tilde{w}(q,\delta u) = 0$. Together with Eqs. (3.7)–(3.11) this implies

$$\sigma_0(q\to\infty) = \kappa q^2 + O(q^4), \quad \kappa>0. \tag{3.14}$$

Since the bending rigidity $\kappa>0$ is always positive [see Eq. (2.32)], Eq. (3.14) states that the interface is stable with respect to perturbations with short wavelengths. The range of validity of Eq. (3.11) reaches up to the microscopic cutoff at $q_{\max} = r_0^{-1}$ set by physical considerations according to which the concept of capillary wavelike fluctuations is valid at most up to wavelengths comparable to the diameter of the fluid particles. Equation (3.14) has the pleasant feature to render this momentum cutoff superfluous. If thermal averages are evaluated with the statistical weight $\exp\{-\beta\mathcal{H}^{(G)}[\tilde{f}(\mathbf{q})]\}$ the increase of $\sigma_0(q)$ for large q implies that the unphysical fluctuations with $q>q_{\max}$ are penalized with such a small statistical weight that the momentum cutoff $q_{\max}$ can be replaced by infinity without significant quantitative errors. As a consequence our approach does not require a quantitatively precise value for $q_{\max}$. We emphasize that this valuable aspect of the present theory depends on its rather detailed description. The positivity of the bending rigidity κ is linked to the distortion of the intrinsic density profile due to the curvature of the interface configuration, i.e., $\rho_H(u)\neq 0$ [see Eqs. (2.16) and (2.31)]. Therefore previous theoretical approaches, which are based only on the intrinsic profile $\rho_0(u)$ for a flat interface, miss the important increase of $\sigma_0(q)$ for large q [14]. According to Eq. (3.14), $\sigma_0(q)$ may contain terms which increase for $q\to\infty$ even stronger than κq^2. These terms correspond to higher-order contributions to the expansion of $\rho_f(u)$ into curvatures of the interface configuration $f(\mathbf{R})$ [Eq. (2.16)] and to additional terms which arise from the transformation to normal coordinates but are not captured by Eq. (2.21). Although knowledge of these terms $O(q^4)$ in $\sigma_0(q)$ would be highly welcome in order to improve the quantitative reliability of the effective interface

Hamiltonian for large values of q, the suppression of fluctuations with small wavelengths is already accomplished by the term κq^2 in $\sigma_0(q)$.

C. Long-wavelength limit

Whereas the approach of $\sigma_0(q)$ towards a finite positive value σ_0 at $q=0$ and the increase of $\sigma_0(q)\sim\kappa q^2$ for large q are, to a large extent, independent of the structure and the form of the interparticle potential, the way in which $\sigma_0(q)$ interpolates between these limiting behaviors depends sensitively on the analytic properties of $w(r)$.

If $w(r\to\infty)$ decays exponentially or faster, $\sigma_0(q\to 0)$ is an analytic function of $\mathbf{q}$ and thus it can be expanded around $\mathbf{q}=0$ into even powers of q:

$$\sigma_0(q\to 0)=\sigma_0+\kappa_0 q^2+O(q^4), \quad \text{short-ranged forces,} \tag{3.15}$$

with

$$\kappa_0=\kappa+\int\int_{-\infty}^{\infty}du\,du'\left(\frac{1}{24}\tilde{w}^{(iv)}(0,u-u')\frac{\partial\rho_0(u)}{\partial u}\frac{\partial\rho_0(u')}{\partial u'}+\tilde{w}''(0,u-u')\rho_H(u)\frac{\partial\rho_0(u')}{\partial u'}+\tilde{w}(0,u-u')\rho_H(u)\rho_H(u')\right), \quad \text{short-ranged forces,} \tag{3.16}$$

where in $d=3$

$$\tilde{w}^{(iv)}(0,u)=\frac{3\pi}{4}\int_0^\infty dR R^5 w(\sqrt{R^2+u^2})<0. \tag{3.17}$$

We emphasize that the amplitude κ_0 of the q^2 term of the small-q behavior [Eq. (3.15)] differs from the amplitude κ of the q^2 term of the large-q behavior [Eq. (3.14)] of $\sigma_0(q)$. This indicates that even for short-ranged forces there is a nontrivial crossover between the asymptotic behaviors $q\to 0$ and $q\to\infty$. Whereas κ is positive [Eq. (2.31)] all three terms forming the integrand of the double integral in Eq. (3.16) are negative so that κ_0 can become negative. Thus the sign of κ_0 depends on the details of the interaction potential $w(r)$ and of the resulting profiles $\rho_0(u)$ and $\rho_H(u)$. This implies that, in marked contrast to the usual ansatz in phenomenological capillary wave theory [23], κ_0 in Eq. (3.16) can be *negative*. Also in this case the q dependences of $\tilde{h}_0(q)$, $\tilde{\kappa}_0^{(H)}(q)$, and $\tilde{\kappa}_0^{(HH)}(q)$ in Eq. (3.11) yield a smooth crossover towards the increase $\sim\kappa q^2,\kappa>0$, for large q. Thus for negative values of $\kappa_0,\sigma_0(q)$ exhibits a *local maximum* at $q=0$ followed by a *global minimum* at $q_{\min}>0$ and an unlimited increase for $q>q_{\min}$. Such a nonmonotonic form of $\sigma_0(q)$ is beyond the predictions of phenomenological capillary wave theories.

Whereas for short-ranged forces $\sigma_0(q)$ can be either a monotonically increasing function with its minimum at $q=0$ or a nonmonotonic function with its minimum at $q_{\min}>0$, for algebraically decaying dispersion forces with $w(r\to\infty)=-Ar^{-(d+\tau)}$, $\tau>1$, the latter nonmonotonic behavior is the rule. Moreover, algebraically decaying interaction potentials induce a *nonanalytic* behavior of $\sigma_0(q)$ for $q\to 0$. This follows from the fact that the moments $\int_{\mathbb{R}^d}d^d r\, r^n w(r)$ do not exist for $n\geqslant\tau$ so that $\tilde{w}^{(iv)}(0,\delta u)$ [Eq. (3.17)] and thus κ_0 [Eq. (3.16)] diverge for $\tau\leqslant 3$. Therefore the expansion of $\sigma_0(q\to 0)$ into powers of q^2 [Eq. (3.15)] breaks down for the physically interesting case of three-dimensional fluids governed by dispersion forces, i.e., $(d,\tau)=(3,3)$ for which $w(r\to\infty)\sim r^{-6}$. Based both on the analytic analysis of the asymptotic behavior of the function $\tilde{w}(\mathbf{q},\delta u)$ and on numerical evaluations of Eq. (3.11) for specific interaction potentials (see below), we find that $\sigma_0(q\to 0)$ is the sum of analytic (a) and nonanalytic (na) terms:

$$\sigma_0(q\to 0)=\sigma_0^{(a)}(q\to 0)+\sigma_0^{(na)}(q\to 0), \tag{3.18}$$

with

$$\sigma_0^{(a)}(q\to 0)=\sum_{i\geqslant 0}\kappa_0^{(i)}q^{2i}=\sigma_0+\kappa_0 q^2+\kappa_0^{(2)}q^4+\cdots, \tag{3.19}$$

where we have used the abbreviations $\kappa_0^{(0)}\equiv\sigma_0$ [Eq. (3.12)] and $\kappa_0^{(1)}\equiv\kappa_0$ [note that for $\tau\leqslant 3\kappa_0$ is not given by Eq. (3.16); see Eq. (3.25)], and

$$\sigma_0^{(na)}(q\to 0)=\sum_{i\geqslant 0}\lambda_0^{(i)}q^{\tau-1+2i}=\lambda_0^{(0)}q^{\tau-1}+\lambda_0^{(1)}q^{\tau+1}+\cdots, \quad \tau\neq 2n+1, \tag{3.20}$$

for $n\in\mathbb{N}_0$. If τ happens to be an odd number $2n+1$, resonances between the corresponding analytic and nonanalytic terms generate nonanalytic contributions $\sim q^{2m}\ln q$ with $2m=2n,2n+2,\ldots$, which replace the power law singularities, yielding

$$\sigma_0^{(na)}(q\to 0)=\sum_{i\geqslant 0}\overline{\lambda}_0^{(i)}q^{\tau-1+2i}\ln q=\overline{\lambda}_0^{(0)}q^{\tau-1}\ln q+\cdots, \quad \tau=2n+1. \tag{3.21}$$

The types of singularities described by Eqs. (3.20) and (3.21) are the same as those obtained within the sharp-kink approximation for the intrinsic interface profile [14(a)]. The first case [Eq. (3.20)] is important for retarded dispersion forces decaying algebraically with $w(r\to\infty)=-Ar^{-7}$, i.e., $\tau=4$. For nonretarded ($\tau=3$) interactions, one finds that the leading term $\overline{\lambda}_0^{(0)}$ is positive for an attractive potential, i.e., $A>0$. Therefore, the surface tension $\sigma_0(q)$ exhibits always a local maximum at $q=0$. This will be discussed in the following.

For the case of three-dimensional fluids governed by dispersion forces, i.e., $(d,\tau)=(3,3)$ these considerations yield

$$\sigma_0(q\to 0)=\sigma_0+\kappa_0 q^2+\overline{\lambda}_0^{(0)}q^2\ln q+O(q^4), \quad \tau=3. \tag{3.22}$$

σ_0 is given by Eq. (3.12). The amplitudes κ_0 and $\bar{\lambda}_0^{(0)}$ are determined by $\tilde{h}_0(q)$, $\tilde{\kappa}_0^{(H)}(q)$, and $\tilde{\kappa}_0^{(HH)}(q)$ [see Eqs. (3.7)–(3.9) and (3.11)]. With

$$\tilde{h}_0(q\to 0)=\tilde{h}_0(0)+\frac{1}{2}\tilde{h}_0''(0)q^2+\gamma_4 q^4+\bar{\gamma}_4 q^4\ln q + O(q^6), \quad \tau=3, \tag{3.23}$$

one has ($\tau=3$)

$$\bar{\lambda}_0^{(0)}=-4\bar{\gamma}_4=\lim_{q\to 0}\frac{1}{q^4\ln q}\int\int_{-\infty}^{\infty}du\,du'\times\left(\tilde{w}(q,\delta u)-\tilde{w}(0,\delta u)-\tilde{w}''(0,u-u')\frac{q^2}{2}\right)\times\frac{\partial\rho_0(u)}{\partial u}\frac{\partial\rho_0(u')}{\partial u'} \tag{3.24}$$

and

$$\kappa_0=\kappa-4\gamma_4+\int\int_{-\infty}^{\infty}du\,du'\times\left(\tilde{w}''(0,u-u')\rho_H(u)\frac{\partial\rho_0(u')}{\partial u'}+\tilde{w}(0,u-u')\rho_H(u)\rho_H(u')\right). \tag{3.25}$$

κ is given by Eq. (2.32). Thus for dispersion forces Eqs. (3.22) and (3.25) replace Eqs. (3.15) and (3.16), respectively.

D. Product approximation

An accurate evaluation of Eqs. (3.11) and (3.22)–(3.25) can be carried out only numerically (see below). However, it is very instructive to provide in addition explicit, albeit approximate, expressions for these quantities. To this end we first introduce dimensionless functions $\bar{\rho}_0(x)$ and $\bar{\rho}_H(x)$ describing the two relevant density profiles:

$$\rho_0(u)=\bar{\rho}-\frac{1}{2}\Delta\rho\,\bar{\rho}_0\left(\frac{u}{\xi}\right), \quad \bar{\rho}_0(x=\pm\infty)=\pm 1 \tag{3.26}$$

and

$$\rho_H(u)=C_H\Delta\rho\,\xi\,\bar{\rho}_H\left(\frac{u}{\xi}\right), \quad \bar{\rho}_H(x=\pm\infty)=0. \tag{3.27}$$

Dimensional analysis shows that in general $\bar{\rho}_0$ depends on u/ξ, r_0/ξ, and $w_0/(k_BT)$ where $\xi^2=(1/2d)\times[\int d^d\mathbf{r}r^2G(r)]/\int d^d\mathbf{r}G(r)$ is the bulk correlation length defined via the second moment of the two-point correlation function $G(r=|\mathbf{r}_1-\mathbf{r}_2|)=\langle\rho(\mathbf{r}_1)\rho(\mathbf{r}_2)\rangle-\langle\rho(\mathbf{r}_1)\rangle\langle\rho(\mathbf{r}_2)\rangle$. r_0 and w_0 set the length and energy scale of the interparticle potential, for example given by Eq. (2.2). For the density functional approach given in Eq. (2.1) one finds $\xi^2=-\rho^2K_T\int d^3\mathbf{r}r^2w(r)$ where

$$K_T=-\frac{1}{V}\left(\frac{\partial V}{\partial p}\right)_{T,N}=\rho^{-2}\left(\frac{\partial^2 f_h(\rho)}{\partial\rho^2}-w^{(0)}\right)^{-1} \tag{3.28}$$

denotes the isothermal compressibility and $\partial^2 f_h(\rho)/\partial\rho^2$ is evaluated at the equilibrium bulk densities at coexistence. For $T\to T_c$ the correlation length $\xi=\xi_0^-t^{-\nu}$, $t=(T_c-T)/T_c$, diverges for $t\to 0$ where ν is a universal bulk exponent, whose value equals 0.5 for the present mean field theory [Eq. (2.1)]. ξ_0^- is a nonuniversal amplitude with $\xi_0^-=r_0/2$ for the model defined by Eqs. (2.2) and (2.3). For temperatures well below T_c the correlation lengths in the liquid $\xi^{(l)}$ and vapor $\xi^{(g)}$ phases differ from each other and from the limiting common value $\xi=\xi_0^-t^{-\nu}$. Although it is straightforward to determine $\xi^{(l)}$ and $\xi^{(g)}$ numerically, we have opted for the advantage of using the following analytic expression:

$$\xi(T)=a(T)\left(1-\frac{T}{T_c}\right)^{-\nu}, \quad a(T)=\xi_0^-\frac{T}{T_c}, \quad \nu=\frac{1}{2}, \tag{3.29}$$

where the amplitude $a(T)$ exhibits a linear temperature dependence. The expression in Eq. (3.29) has the virtue of fulfilling the relations $\xi^{(l)}>\xi(T)>\xi^{(g)}$ and will be used in the following whenever an explicit expression for the correlation length is needed. Moreover, it has the appealing property that at the triple point $T_{\rm tr}\simeq(2/3)T_c$ the correlation length $\xi(T_{\rm tr})\approx 0.58r_0$ is of the order of the microscopic cutoff length r_0 which is assumed to be larger than but comparable to the diameter of the particles. For temperatures below $T_{\rm tr}$ —where no fluid interface exists—the model defined by Eq. (2.1) ceases to be applicable because it does not capture the freezing transition, which would require a more sophisticated version of the density functional.

In the limit $T\to T_c$ the dependences of $\bar{\rho}_0(x)$ on r_0/ξ and $w_0/(k_BT)$ drop out and $\bar{\rho}_0(x)$ reduces to a universal function $\bar{\rho}_0(x)$ whose mean field approximation is given by

$$\bar{\rho}_0(x)=\tanh\frac{x}{2}. \tag{3.30}$$

For a qualitative estimate this expression can be useful even away from T_c; a quantitatively reliable expression requires to solving Eq. (2.8) numerically. Analogous information about $\rho_H(u)$ is presently not available. In the spirit of the above reasoning we adopt a similar scaling form for ρ_H [Eq. (3.27)]. The correct naive dimension is taken into account by the amplitudes $\Delta\rho$ and ξ, assuming that they set the relevant scales. The dimensionless amplitude $C_H>0$ is fixed by the requirement $\int_{-\infty}^{\infty}dx\,\bar{\rho}_H(x)=1$. Therefore, its value depends on the definition of the interface [Eq. (2.5)]. Regrettably, within the density functional used here, there are no explicit results available for the profile $\bar{\rho}_H(x)$ or for the amplitude C_H. We assume that C_H is temperature independent and that its value is smaller than 1 because the distortion due to the curvature is expected to be not larger than the density difference $\Delta\rho$ itself. For example, within the double-parabola ap-

proximation of Landau theory one finds $C_H=0.25$. In order to proceed, for actual calculations we adopt the following form of the profile:

$$\overline{\rho}_H(x)=\frac{1}{4\pi}\frac{x\sinh x/2}{\cosh^2 x/2}, \tag{3.31}$$

which is positive in accordance with the physical arguments given in the paragraph following Eq. (2.20).

The functions $\tilde{h}_0(q)$, $\tilde{\kappa}_0^{(H)}(q)$, and $\tilde{\kappa}_0^{(HH)}(q)$ can be expressed in terms of these scaling functions. Starting from Eq. (3.7) for the double integral one can apply the following—as we call it—product approximation which is valid in the case $\xi \gg r_0$:

$$\begin{aligned}\tilde{h}_0(q)&=-\frac{1}{16}(\Delta\rho)^2\frac{r_0}{\xi}\int\int_{-\infty}^{\infty}dx\,dx'\,\tilde{w}(\mathbf{q},xr_0)\\&\quad\times\frac{\partial\overline{\rho}_0(x'+x(r_0/\xi))}{\partial x'}\frac{\partial\overline{\rho}_0(x')}{\partial x'}\\&=-\frac{1}{16}(\Delta\rho)^2\frac{r_0}{\xi}\int\int_{-\infty}^{\infty}dx\,dx'\,\tilde{w}(\mathbf{q},xr_0)\\&\quad\times\left(\frac{\partial\overline{\rho}_0(x')}{\partial x'}\right)^2+O((r_0/\xi)^3)\\&=-\frac{1}{16}(\Delta\rho)^2\frac{1}{\xi}\left(\int_{-\infty}^{\infty}du\,\tilde{w}(\mathbf{q},u)\right)\int_{-\infty}^{\infty}dx\left(\frac{\partial\overline{\rho}_0(x)}{\partial x}\right)^2\\&\quad+O((r_0/\xi)^3).\end{aligned} \tag{3.32}$$

For the second equation we used the property that $\tilde{w}(q,u)$ is an even function of u peaked at $u=0$. With the *three*-dimensional Fourier transform $\tilde{w}(\mathbf{Q})=\tilde{w}(|\mathbf{Q}|)$ of the interparticle potential $w(r)$,

$$\tilde{w}(\mathbf{Q})=\int_{\mathbb{R}^3}d^3r\,e^{-i\mathbf{Q}\cdot\mathbf{r}}w(r), \tag{3.33}$$

one has, for $\mathbf{Q}=(\mathbf{q},0)$ [see Eq. (3.6)],

$$\int_{-\infty}^{\infty}du\,\tilde{w}(q,u)=\tilde{w}(|\mathbf{Q}|=q)=\frac{4\pi}{q}\int_0^{\infty}dr\,rw(r)\sin qr. \tag{3.34}$$

This leads to the approximation

$$\tilde{h}_0(q)\simeq-\frac{(\Delta\rho)^2}{16\,\xi}I_0\tilde{w}(q)+O((r_0/\xi)^3), \tag{3.35}$$

with the dimensionless integral

$$I_0=\int_{-\infty}^{\infty}dx\left(\frac{\partial\overline{\rho}_0(x)}{\partial x}\right)^2>0. \tag{3.36}$$

The comparison of the product approximation with the full numerical evaluation of $\tilde{h}_0(q)$ [Eq. (3.7)] reveals that the difference between them is less than 10% for the full temperature range and typically less than 1% for $\xi>10r_0$. Thus, the product approximation in Eq. (3.35) yields a good overall picture of the behavior of $\sigma_0(q)$. A more detailed comparison will be presented in Sec. III E. Along the same line of arguments one finds

$$\tilde{\kappa}_0^{(H)}(q)\simeq-\frac{1}{2}C_H(\Delta\rho)^2\xi I_H\tilde{w}(q) \tag{3.37}$$

and

$$\tilde{\kappa}_0^{(HH)}(q)\simeq-C_H^2(\Delta\rho)^2\xi^3I_{HH}\tilde{w}(q), \tag{3.38}$$

with the dimensionless integrals

$$I_H=\int_{-\infty}^{\infty}dx\,\overline{\rho}_H(x)\frac{\partial\overline{\rho}_0(x)}{\partial x}>0 \tag{3.39}$$

and

$$I_{HH}=\int_{-\infty}^{\infty}dx[\overline{\rho}_H(x)]^2>0. \tag{3.40}$$

For the functional forms of $\overline{\rho}_0(x)$ and $\overline{\rho}_H(x)$ as given by Eqs. (3.30) and (3.31), respectively, one obtains $I_H=1/12$, $I_0=2/3$, and $I_{HH}=1/36+1/(3\pi^2)$.

Thus, within this product approximation, the momentum-dependent surface tension [Eq. (3.11)] is given as

$$\begin{aligned}\sigma_0(q)&\simeq(\sigma_0-\kappa_0^{(H)}q^2)\frac{\tilde{w}(q)-\tilde{w}(0)}{\frac{1}{2}\tilde{w}''(0)q^2}\\&\quad+\left(\kappa-\kappa_0^{(HH)}\frac{\tilde{w}(q)}{\tilde{w}(0)}\right)q^2+O(q^4)\end{aligned} \tag{3.41}$$

with $\tilde{w}''(0)>0$, $\tilde{w}(0)<0$ [Eq. (3.33)],

$$\sigma_0=-2\tilde{h}_0''(0)\simeq\frac{1}{8}\tilde{w}''(0)\frac{(\Delta\rho)^2}{\xi}I_0>0, \tag{3.42}$$

$$\kappa_0^{(H)}=-\tilde{\kappa}_0^{(H)''}(0)\simeq\frac{1}{2}\tilde{w}''(0)(\Delta\rho)^2C_H\xi I_H>0, \tag{3.43}$$

$$\kappa_0^{(HH)}=\tilde{\kappa}_0^{(HH)}(0)\simeq-\tilde{w}(0)(\Delta\rho)^2C_H^2\xi^3I_{HH}>0, \tag{3.44}$$

and, without invoking the product approximation [see Eq. (3.32)],

$$\kappa=(\Delta\rho)^2C_H^2\xi^3\int_{-\infty}^{\infty}dx[\overline{\rho}_H(x)]^2\left.\frac{\partial^2f_h(\rho)}{\partial\rho^2}\right|_{\rho=\rho_0(u=x\xi)}>0. \tag{3.45}$$

Within this product approximation the momentum dependence of $\sigma_0(q)$ is determined by the *three*-dimensional Fourier transform $\tilde{w}(\mathbf{Q})$ of the interparticle potential $w(r)$ evaluated for the absolute value of the lateral momentum $\mathbf{q}$. For short-ranged forces $\tilde{w}(q)$ is analytic around $\mathbf{q}=0$ so that

$$\tilde{w}(q\to0)=\sum_{i=0}^{\infty}\frac{1}{(2i)!}\tilde{w}^{(2i)}(0)q^{2i},\quad\text{short-ranged forces,} \tag{3.46}$$

with

$$\tilde{w}^{(2i)}(0)=(-1)^i\frac{4\pi}{2i+1}\int_0^\infty dr\, r^{2i+2}w(r) \tag{3.47}$$

in $d=3$. If $w(r)$ decays algebraically as $w(r\to\infty)=-Ar^{-(d+\tau)}$, the expansion of $\tilde{w}(q\to 0)$ contains analytic terms $\sim q^{2i}$, $i\in\mathbb{N}_0$, whose amplitudes are, however, given by $[1/(2i)!]\tilde{w}^{(2i)}(0)$, only for $2i<\tau$, and nonanalytic terms. The leading nonanalytic term is given by

$$[\tilde{w}(q\to 0)]_{na}=\frac{-A\pi^{d/2+1}2^{-\tau}q^\tau}{\sin[\pi(\tau/2+1)]\Gamma((\tau+d)/2)\Gamma(\tau/2+1)}. \tag{3.48}$$

The subdominant nonanalytic terms depend on the subdominant decay of $w(r)$. For $\tau=2n$ resonances with the analytic terms lead to singularities $\sim q^{2n}\ln q$ instead of algebraic ones. Together with Eq. (3.41) these results show a remarkable difference to Eqs. (3.19)–(3.23). For the case $(d,\tau)=(3,3)$ one has

$$\tilde{w}(q\to 0)=\tilde{w}(0)+\frac{1}{2}\tilde{w}''(0)q^2-\frac{\pi^2}{12}Aq^3+\tilde{w}_4q^4+\tilde{w}_5q^5+O(q^6),\quad \tau=3. \tag{3.49}$$

The first two terms are given by Eq. (3.47) whereas similar explicit formulas for $\tilde{w}_4$ and $\tilde{w}_5$ are not available. Inserting Eq. (3.49) into Eq. (3.41) leads, in contrast to Eq. (3.22), to the form

$$\sigma_0(q\to 0)=\sigma_0+\eta_0^{(0)}q+\kappa_0q^2+\eta_0^{(1)}q^3+O(q^4),\quad \tau=3, \tag{3.50}$$

of $\sigma_0(q\to 0)$ with the following explicit expressions for the corresponding coefficients as obtained within the product approximation:

$$\eta_0^{(0)}=-\frac{\pi^2}{6}A\frac{\sigma_0}{\tilde{w}''(0)}<0, \tag{3.51}$$

$$\kappa_0=\kappa-\kappa_0^{(H)}-\kappa_0^{(HH)}+2\frac{\sigma_0}{\tilde{w}''(0)}\tilde{w}_4, \tag{3.52}$$

and

$$\eta_0^{(1)}=2\frac{\sigma_0}{\tilde{w}''(0)}\tilde{w}_5+\frac{\pi^2}{6}A\frac{\kappa_0^{(H)}}{\tilde{w}''(0)} \tag{3.53}$$

[see Eqs. (3.41)–(3.45), (3.47), and (3.49)]. Thus the product approximation yields a stronger singularity of $\sigma_0(q\to 0)$ [$\sim q$, Eq. (3.50)] than the full theory [$\sim q^2\ln q$, Eq. (3.22)]. As discussed below the full result for $\sigma_0(q)$ exhibits a linear behavior $\sim q$ for $q\to 0$ which ultimately crosses over to the behavior $\sim q^2\ln q$. For increasing values of ξ, for which the quality of the product approximation improves, this crossover to the behavior $\sim q^2\ln q$ occurs for smaller values of q. In this sense the product approximation is a valuable approximation although it misses the ultimate singular behavior $\sim q^2\ln q$ for $q\to 0$.

The most important feature of the above results is that for the generic case of fluids governed by dispersion forces decaying $\sim r^{-6}$ the coefficient $\eta_0^{(0)}$ is always *negative*. Remarkably, to a large extent the value of $\eta_0^{(0)}$ depends only on the amplitude A of this asymptotic decay because $\sigma_0/\tilde{w}''(0)$ is independent of $\tilde{w}''(0)$ [Eq. (3.42)]. The actual form of $w(r)$, besides its asymptotic behavior for $r\to\infty$, enters only indirectly via $\Delta\rho$, ξ, and $\overline{\rho}_0(x)$. The negative value of $\eta_0^{(0)}$ implies that within the product approximation $\sigma_0(q)$ attains linearly a local maximum at $q=0$, exhibits a minimum at $q_{\min}>0$, and crosses over to the increase described by Eq. (3.14). In contrast to $\eta_0^{(0)}$ the signs of κ_0 and $\lambda_0^{(1)}$ are not fixed so that it depends on the specific system whether the terms $\sim q^2$ and $\sim q^3$ or only even higher ones accomplish the formation of the minimum of $\sigma_0(q)$. As mentioned after Eq. (3.53), for values $-qr_0\ln qr_0<r_0/\xi$ the product approximation [Eq. (3.50)] is no longer valid and there is a crossover to the ultimate asymptotic behavior $q\to 0$ as given by Eq. (3.22).

For the interaction potential in Eq. (2.2) one has $A=w_0r_0^6$ and $\tilde{w}(q)=\tilde{w}(0)(1+qr_0)e^{-qr_0}$ with $\tilde{w}(0)=-w^{(0)}=-\pi^2r_0^3w_0/4<0$, $\tilde{w}''(0)=-\tilde{w}(0)r_0^2>0$, $\tilde{w}_4=\tilde{w}(0)r_0^4/8<0$, $\tilde{w}_5=\tilde{w}(0)r_0^5/30<0$, and $\int d^3\mathbf{r}r^2w(r)=-3\tilde{w}''(0)$. The signs of κ_0 and $\eta_0^{(1)}$ depend on the shape of the profiles $\overline{\rho}_0(x)$ and $\overline{\rho}_H(x)$, the amplitude C_H, and temperature:

$$\kappa_0=-\tilde{w}(0)(\Delta\rho)^2\frac{r_0^4}{\xi}\left[C_H^2I_\kappa\left(\frac{\xi}{r_0}\right)^4-\frac{1}{2}C_H\left(\frac{\xi}{r_0}\right)^2I_H-\frac{1}{32}I_0\right], \tag{3.54}$$

with the dimensionless integral

$$I_\kappa=-\frac{1}{\tilde{w}(0)}\int_{-\infty}^{\infty}dx\left(\tilde{w}(0)+\left.\frac{\partial^2f_h(\rho)}{\partial\rho^2}\right|_{\rho_0(x\xi)}\right)[\overline{\rho}_H(x)]^2>0. \tag{3.55}$$

For the form of the profile $\overline{\rho}_H(x)$ as given by Eq. (3.31) and by using Eqs. (2.1) and (2.3) it turns out numerically that for temperatures above the triple point $T_{\rm tr}\simeq(2/3)T_c$ the integral in Eq. (3.55) can be approximated by

$$I_\kappa=\frac{1}{2}\left(\frac{r_0}{\xi}\right)^2I_{HH}, \tag{3.56}$$

which amounts to replacing in the factor $\tilde{w}(0)+[\partial^2f_h(\rho)/\partial\rho^2]=\xi^{-2}(T,\rho)\tilde{w}''(0)/2$ entering the integrand in Eq. (3.55) the actual correlation length by its aprroximate form $\xi(T,\rho)\simeq a(T)t^{-1/2}$ with the amplitude $a(T)=\xi_0^-T/T_c$ which depends on T but not on ρ [see Eq. (3.29)]. The error of the approximation is less than 20% and is well within the upper and lower bounds which one obtains by using the correlation length in the liquid and vapor phases, respectively, in the formula (3.56). Thus, we regard the numerical error of this approximation to be smaller than the uncertainty induced by the definition of the profile $\rho_H(u/\xi)$ itself.

Using the same kind of reasoning leading to the expression in Eq. (3.56) one finds, for the bending rigidity [Eq. (3.45)],

$$\kappa=\kappa_0^{(HH)}\left(1+\frac{1}{2}\frac{r_0^2}{\xi^2}\right) \tag{3.57}$$

[see Eq. (3.44)].

From Eqs. (3.54)–(3.56) and from the values for I_H, I_0, and I_{HH} given below Eq. (3.40) as well as from Eq. (3.29) it follows that the coefficient κ_0 in Eq. (3.54) is negative for all temperatures if $C_H<C_H^*=1/(12I_{HH})\simeq 1.35$. For $C_H>C_H^*$ the coefficient κ_0 is negative for temperatures between the triple point $T_{\rm tr}\simeq\frac{2}{3}T_c$ and a temperature $T^*(C_H)$ and κ_0 is positive within the temperature range $T^*(C_H)<T<T_c$. (For the model fluid considered here the critical point is given within the present density functional theory by $k_BT_c\simeq 0.09w^{(0)}r_0^{-3}\simeq 0.22w_0$ and $\rho_c r_0^3=0.249$.) The coefficient κ_0 changes sign at

$$\frac{T^*}{T_c}=\frac{1}{C_H-C_H^2/C_H^*}\left(1-\sqrt{1-2C_H+2C_H^2/C_H^*}\right),$$

$$C_H>C_H^*\simeq 1.35. \tag{3.58}$$

This result demonstrates that independent model calculations for the hitherto unknown amplitude C_H would be highly welcome because its actual value has significant repercussions on the behavior of $\sigma(q)$.

Within our model the coefficient $\eta_0^{(1)}$ [Eq. (3.53)] reduces to

$$\eta_0^{(1)}=\frac{\pi^2}{12}w_0r_0^8\frac{(\Delta\rho)^2}{\xi}\left[C_HI_H\left(\frac{\xi}{r_0}\right)^2-\frac{1}{40}I_0\right]. \tag{3.59}$$

Equation (3.59) implies that for $C_H>\frac{4}{15}$ the coefficient $\eta_0^{(1)}$ is positive for $T_{\rm tr}<T<T_c$. For $C_H<\frac{4}{15}$ the coefficient $\eta_0^{(1)}$ is positive within the temperature range $(1-\frac{5}{4}C_H)T_c<T<T_c$ but negative for $T_{\rm tr}<T<(1-\frac{5}{4}C_H)T_c$. From this analysis we infer that typically the formation of the minimum of $\sigma_0(q)$, i.e., the increase of $\sigma_0(q)$, for large q is accomplished by the term $\sim q^2$ [see Eq. (3.50)] and provided C_H is sufficiently large and the temperature sufficiently high.

Finally, for the interaction potential discussed above [Eq. (2.2)] we quote the full expression for $\sigma_0(q)$ as obtained from the product approximation given by Eq. (3.41):

$$\begin{aligned}\frac{\sigma_0(q)}{\sigma_0}=&\left[2-C_H\left(\frac{\xi}{r_0}\right)^2y^2\right]\frac{1-(1+y)e^{-y}}{y^2}\\&+0.74C_H^2\left(\frac{\xi}{r_0}\right)^2y^2\left[\frac{1}{2}+\left(\frac{\xi}{r_0}\right)^2[1-(1+y)e^{-y}]\right]\\&+O(y^4)=1-\frac{2}{3}y+\frac{1}{2}\left[(0.74C_H^2-C_H)\left(\frac{\xi}{r_0}\right)^2\right.\\&\left.-\frac{1}{2}\right]y^2+\frac{1}{3}\left[C_H\left(\frac{\xi}{r_0}\right)^2-\frac{1}{5}\right]y^3+O(y^4),\quad y=qr_0.\end{aligned} \tag{3.60}$$

This result can be written in terms of the variable $\zeta=q\xi$ so that

$$\begin{aligned}\frac{\sigma_0(q)}{\sigma_0}=&1+\frac{1}{2}(0.74C_H^2-C_H)\zeta^2+\frac{0.74}{2}C_H^2\zeta^4\\&-\left(\frac{2}{3}\zeta-\frac{1}{3}C_H\zeta^3+\frac{0.74}{3}C_H^2\zeta^5\right)\frac{r_0}{\xi}+O\left(\left(\frac{r_0}{\xi}\right)^2\right).\end{aligned} \tag{3.61}$$

In the limit $\xi\to\infty$ the contributions $\sim r_0/\xi$ and $O((r_0/\xi)^2)$ vanish and $\sigma_0(q)/\sigma_0$ reduces to a function of ζ only, i.e., $1+\frac{1}{2}(0.74C_H^2-C_H)\zeta^2+O(\zeta^4)$ which increases (decreases) as function of ζ for $C_H>1.35$($C_H<1.35$). The ultimate increase for large values of ζ in the case $C_H<1.35$ is accomplished by terms $O(\zeta^4)$ not captured by the present expansion. Although we neglect contributions $O(\zeta^4)$ in Eq. (3.61), we keep all terms $\sim\zeta^4$ resulting from the expansion of the terms given explicitly in the first part of Eq. (3.60) in order to maintain the qualitative functional form of $\sigma_0(q)$, in particular, the increase for $\zeta\gg 1$, even if $0.74C_H<1$. We note that in the limit $r_0/\xi\to 0$ $\sigma_0(q)$ turns into an *analytic* limiting function of $\zeta=q\xi$. This is not only true within the product expansion [Eq. (3.61)] but also for the full theory, because the latter reduces to the product approximation in the limit $r_0/\xi\to 0$.

We emphasize that, inspite of the fact that within the product approximation for r_0/ξ finite $\sigma_0(q\to 0)$ does not exhibit the correct singular behavior $q^2\ln q$, Eqs. (3.60) and (3.61) represent useful analytic expressions which provide a good overall account of the behavior of $\sigma_0(q)$.

E. Numerical analysis and temperature dependence

The explicit results given above allow one to obtain a transparent view of the overall behavior of $\sigma_0(q)$, of its parametric dependence on various features of the intrinsic profile, and of its temperature dependence. This advantage is based on the product approximation described in Eq. (3.32). By carrying out a full numerical analysis for the model considered above we are able to assess the reliability of this approximation. To this end we compare Eq. (3.12) with Eq. (3.42) and Eq. (3.25) with Eq. (3.54). We find that the full numerical results agree with the product approximation to within 10% as long as $\xi>r_0$, i.e., for $T>0.83T_c$ [see Eq. (3.29)] which is slightly above the triple point $T_{\rm tr}\simeq 0.67T_c$.

In Fig. 3 we compare the full form of $\sigma_0(q)$ as described by Eq. (3.11) with its approximate form given by Eq. (3.41) for two limiting cases: $r_0/\xi=1$ (i.e., $T>0.83T_c$) close to the triple point and $r_0/\xi=0.1$ (i.e., $t=2.5\cdot 10^{-3}$) close to T_c. We find that in both cases the qualitative functional form of $\sigma_0(q)$ is captured well by the product approximation. In particular, the position $q_{\rm min}$ of the minimum and the increase of $\sigma_0(q)$ for $qr_0\geqslant 2$ are in good agreement with the numerical evaluation of the full form, although the product approximation overestimates the depth of the minimum. This overestimation is linked to the fact that the product approximation yields a behavior $\sigma_0(q\to 0)-\sigma_0=\eta_0^{(0)}q$, $\eta_0^{(0)}<0$, instead of the actual behavior $\sigma_0(q\to 0)-\sigma_0=\overline{\lambda}_0^{(0)}q^2\ln q$, $\overline{\lambda}_0^{(0)}>0$, which leads to a less pronounced decrease of $\sigma_0(q)$ and is the same kind of singularity at $q=0$ as predicted by the sharp-kink approximation [14].

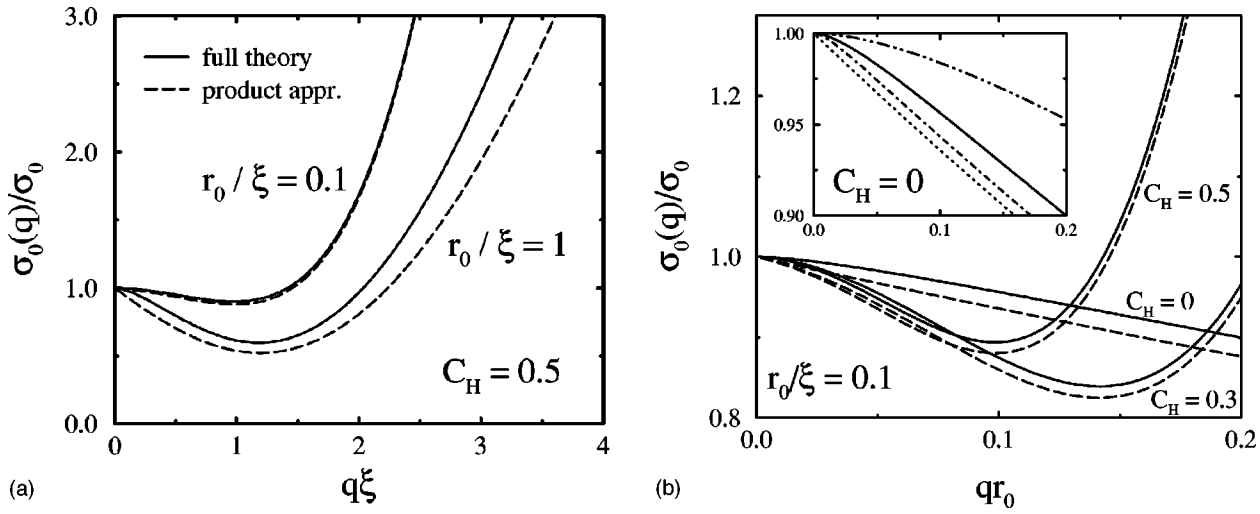

FIG. 3. (a) Normalized momentum-dependent surface tension $\sigma_0(q)/\sigma_0(0)$ as given by Eq. (3.11) (solid curves) and its product approximation (dashed curves) given by Eq. (3.41) for $r_0/\xi=1$ close to the triple point and for $r_0/\xi=0.1$ close to the critical point. The data correspond to the model defined by Eqs. (2.1)–(2.3) where r_0 denotes the diameter of the fluid particles and ξ the bulk correlation length [see Eq. (3.29)]. The interface profiles $\rho_0(u)$ and $\rho_H(u)$ are given by Eqs. (3.26), (3.27), (3.30), and (3.31) with $C_H=0.5$. The numerical results for the full theory are in accordance with the behavior of $\sigma_0(q\to 0)$ as given by Eq. (3.22) and of $\sigma_0(q\to\infty)$ as given by Eq. (3.14). For $q\to 0$ to leading order $\sigma(q)$ decreases as $\overline{\lambda}_0^{(0)}q^2\ln q$ whereas the product approximation predicts a decrease as $\eta_0^{(0)}q$. However, for $q\xi$ sufficiently large the actual decrease $\sim q^2\ln q$ crosses over to the linear decrease $\sim q$ (see the data for $r_0/\xi=1$). As expected, in the limit $r_0/\xi\to 0$ the full expression for $\sigma_0(q)$ reduces to the one predicted by the product approximation, which in this limit turns into an *analytic* limiting function of $\zeta=q\xi$ [see Eq. (3.61)]. Accordingly the term $\eta_0^{(0)}q=(\eta_0^{(0)}/\xi)\zeta$ vanishes in the limit $\xi\to\infty$. The opposite limit $r_0/\xi\to\infty$ corresponds to the sharp-kink approximation which leads to the singularity $q^2\ln q$. For any finite value of r_0/ξ the full expression for $\sigma_0(q)$ has the same leading singularity as predicted by the sharp-kink approximation. Whereas the full expression for $\sigma_0(q)$ contains the sharp-kink approximation as a limiting case, the product approximation cannot capture this case because it is constructed to capture the opposite case. Both the full theory and the product approximation render a minimum of $\sigma_0(q)$ whose temperature dependence is shown in Fig. 4 as a function of r_0/ξ. (b) Normalized momentum-dependent surface tension $\sigma_0(q)/\sigma_0(0)$ for $r_0/\xi=1$ and $C_H=0$, 0.3, and 0.5 as function of qr_0 within the full theory (solid lines) and the product approximation (dashed lines). For increasing amplitudes C_H of the distortion $\rho_H(u)$ of the density profile due to its curvature the location of the minimum is shifted towards smaller values of q and becomes more shallow. For finite values of C_H the behavior of $\sigma_0(q)$ at small q is numerically dominated by the quadratic curvature contribution $\kappa_0 q^2$ [see Eqs. (3.22) and (3.50)]; for $C_H<1.35$ the coefficient is always negative. On this scale the leading singular behavior $\sim q^2\ln(qr_0)$ becomes visible only for $C_H=0$ (inset). The inset shows the behavior of the full expression for $\sigma_0(q)$ for $r_0/\xi=0$ (dotted line), $r_0/\xi=0.02$ (dash-dotted line), $r_0/\xi=0.1$ (solid line), and $r_0/\xi=1$ (dash-double-dotted line). For $-qr_0\ln(qr_0)>r_0/\xi$ one can clearly see a linear decrease of $\sigma_0(q)$ as predicted by the product approximation whereas for $-qr_0\ln(qr_0)<r_0/\xi$ there is a crossover to the singularity $\sim q^2\ln(qr_0)$ of the full theory.

Figure 3(a) corresponds to a fixed amplitude $C_H=0.5$ of the profile $\rho_H(u)$. For smaller values of C_H the minimum is deeper and located at larger values of $q_{\min}$ [Fig. 3(b)]. Figure 3(a) demonstrates that in the limit $r_0/\xi\to 0$, $\sigma_0(q)$ reduces to an *analytic* limiting function of $\zeta=q\xi$, which is proportional to ζ^2 for small ζ with a negative coefficient for $C_H<1.35$ [see Eq. (3.61)]. In the limit $r_0/\xi\to 0$ the full expression for $\sigma_0(q)$ reduces to the one obtained within the product approximation. On the other hand, as function of qr_0 the inset of Fig. 3(b) shows the crossover from the linear momentum dependence, as predicted by the product approximation, to the asymptotic behavior $q^2\ln qr_0$ for $q\to 0$. For $r_0/\xi=0$ the linear decrease of $\sigma_0(q)$ is valid for all values of q whereas for $r_0/\xi>0$ it can be observed only for $-qr_0\ln qr_0>r_0/\xi$.

From Fig. 3 one infers that $\sigma_0(q)$ is a nonmonotonic function forming a minimum at $q_{\min}$. Figure 4 shows the temperature dependence of the position and of the depth of this minimum in terms of the inverse correlation length within the physically accessible temperature range between the triple point at $T_{\rm tr}\simeq\frac{2}{3}T_c$ (i.e., $r_0/\xi\simeq 1.73$) and T_c (i.e., $r_0/\xi=0$). The data (solid line) correspond to the full theory for the model studied in Fig. 3. Within the product approximation (dashed line) upon approaching T_c the minimum of $\sigma_0(q)$ disappears by shifting its position towards $q=0$ according to

$$q_{\min}\sim\frac{1}{\xi^a}\sim t^{a/2},\quad t=1-\frac{T}{T_c}\to 0, \tag{3.62}$$

and by becoming more shallow, i.e.,

$$1-\sigma_0(q_{\min})/\sigma_0\sim t^{a-1}. \tag{3.63}$$

The exponent is given by $a=1$ with $1-\sigma_0(q_{\min})/\sigma_0=O(1)$ for $C_H<C_H^*=1.35$ and $a=2$ for $C_H>C_H^*$ This disappearence of the minimum in $\sigma_0(q)$ for $T\to T_c$ is in accordance with the expectation that near T_c not only the bulk properties but also the interfacial properties can be described by a *local* theory (i.e., based on the Landau-Ginzburg-Wilson Hamiltonian) which does not provide a nonmonotonic behavior of $\sigma_0(q)$.

The product approximation describes the location and the depth of the minimum remarkably well for $C_H<C_H^*$. How-

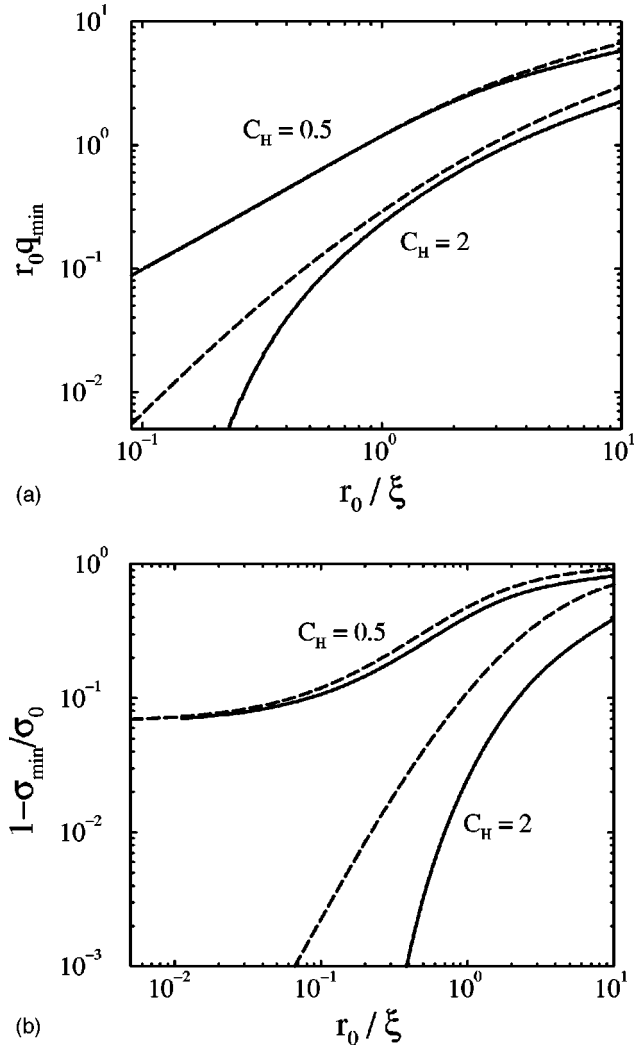

FIG. 4. Temperature dependence of (a) the position, $q_{\min}$, and (b) the depth, $1-\sigma_0(q_{\min})/\sigma_0(0)$, of the minimum of $\sigma_0(q)$ for the same model as in Fig. 3 [Eq. (3.11)] with $C_H=0.5$ and $C_H=2$. The full theory (solid line) is described remarkably well by the product approximation (dashed line) for $C_H<C_H^*$, whereas for $C_H=2$ the asymptotic behavior $\sim q^2 \ln q$ of $\sigma_0(q)$ yields an exponential behavior for the vanishing of these quantities instead of an algebraic one. For $t=(T_c-T)/T_c \to 0$, i.e., $\xi \to \infty$, the position of the minimum $q_{\min}$ vanishes $\sim \xi^{-1}$ and the depth $1-\sigma_0(q_{\min})/\sigma_0(0)$ reaches a constant value for $C_H<C_H^* \simeq 1.35$ whereas for $C_H>C_H^*$ both vanish exponentially as function of ξ. The disappearence of the minimum for $t \to 0$ is in accordance with the expectation that upon approaching T_c the interfacial structures attain universal properties which can be described by a *local* theory within which the range of the forces is zero on the scale of the correlation length so that the phenomenological capillary-wave theory is applicable which does not provide a nonmonotonic behavior of $\sigma_0(q)$. In (a) and (b), due to $T>T_{\rm tr}$, the physically accessible range for r_0/ξ is given by $(r_0/\xi)_{\max}=\sqrt{3} \simeq 1.73$.

ever, for instance, for $C_H=2$ within the full theory there is a crossover to an exponential vanishing of the position and of the depth of the minimum,

$$q_{\min} \sim e^{-c\xi}, \quad 1-\sigma_0(q_{\min})/\sigma_0 \sim e^{-\bar{c}\xi}, \tag{3.64}$$

in accordance to the asymptotic behavior of $\sigma_0(q)$ given by Eq. (3.22).

F. Comparision with other theories

It is instructive to compare the present theory with previous efforts to determine the effective interface Hamiltonian. To this end we do not consider the full form of $\mathcal{H}[f]$ as derived in Sec. II C but confine the discussion to the various corresponding Gaussian approximations.

In the so-called sharp-kink approximation the intrinsic density profile is taken as $\rho^{(\rm sk)}(u)=\rho_l-\Delta\rho\Theta(u)$ with the Heaviside function $\Theta(u)$ so that $\partial\rho_0^{(\rm sk)}(u)/\partial u=-\Delta\rho\,\delta(u)$ (see Sec. II C) and $\rho_H(u)\equiv 0$. In this special case the present theory reduces to the Hamiltonian given in Eq. (2.42) as obtained in Ref. [14]:

$$\mathcal{H}^{(\rm sk)}[f(\mathbf{R})]=\frac{1}{2}mG\Delta\rho\int_A d^2R[f(\mathbf{R})]^2 - \frac{1}{2}(\Delta\rho)^2\int\int_A d^2R\,d^2R'\int_0^\infty dz \times\int_0^{f(\mathbf{R}')-f(\mathbf{R})} dz'\,w(|\mathbf{r}'-\mathbf{r}|). \tag{3.65}$$

Within the Gaussian approximation this result leads to

$$\sigma_0^{(\rm sk)}(q)=(\Delta\rho)^2\frac{\tilde{w}(q,0)-\tilde{w}(0,0)}{q^2}, \tag{3.66}$$

with $\sigma_0^{(\rm sk)}(q\to\infty)=0$, and, for the model potential given by Eq. (2.2), to

$$\sigma_0^{(\rm sk)}(q\to 0)=\sigma_0+\frac{\pi}{32}w_0 r_0^6(\Delta\rho)^2\left[q^2\ln\frac{qr_0}{2}-\left(\frac{3}{4}-C\right)q^2\right], \tag{3.67}$$

where $C\sim 0.5772$ is Euler's constant. The present theory and its sharp-kink approximation have in common that for fluids governed by dispersion forces they predict a maximum of $\sigma_0(q)$ at $q=0$ which is attained via the singular momentum dependence $\sim q^2\ln(qr_0)$. However, the sharp-kink approximation yields a monotonic decrease of $\sigma_0(q)$ and thus fails to predict the increase of $\sigma_0(q)$ for large q and thus the formation of a minimum at $q_{\min}>0$. Therefore we conclude that the smooth variation of the intrinsic density profile and its distortion due to the capillary waves are responsible for the formation of a nontrivial minimum.

The present theory differs qualitatively from the classical capillary wave theory which in its simplest and most commonly used version corresponds to a square-gradient theory, i.e., $\mathcal{H}=\frac{1}{2}\sigma_0\int d^2R[\nabla f(\mathbf{R})]^2$, so that $\sigma_0(q)$ is constant. A more sophisticated but phenomenological ansatz follows from expanding the Fourier transformed Helfrich Hamiltonian into powers of q [12,13], leading to $\sigma_0(q)=\sigma_0+\kappa q^2+O(q^4)$ with $\kappa>0$ [23]. If one assigns the proper values of σ_0 and κ as obtained by the present theory, this phenomenological capillary-wave theory agrees with the present theory for large q, i.e., $q \gg \xi$. However, this ansatz fails to capture the formation of the minimum of $\sigma_0(q)$ at $q_{\min}>0$ as well as the singularity $\sim q^2\ln(qr_0)$ of $\sigma_0(q)$ at $q=0$. Therefore, as shown in Fig. 5, the Helfrich Hamil-

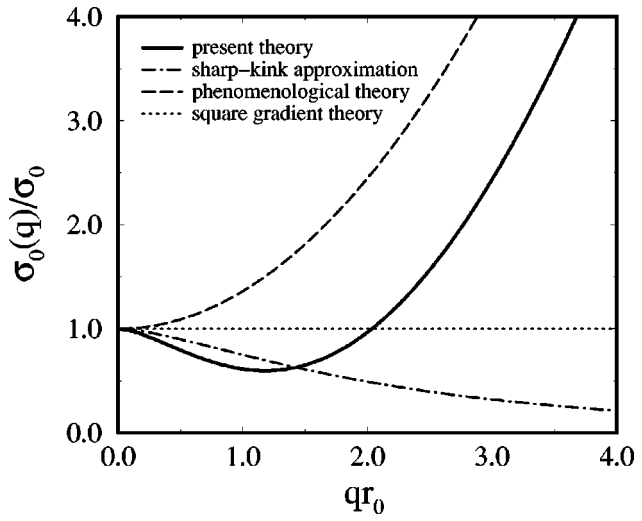

FIG. 5. Comparision of the present theory for $\sigma_0(q)$ [Eq. (3.11), solid curve as shown already in Fig. 3] with the predictions of the simple square-gradient theory $\mathcal{H}=\frac{1}{2}\sigma_0\int d^2R[\nabla f(\mathbf{R})]^2$ (dotted curve), the phenomenological capillary-wave theory [23] corresponding to $\sigma_0(q)/\sigma_0=1+(\kappa/\sigma_0)q^2$ (dashed curve), and the sharp-kink approximation [14] of the present theory (dash-dotted curve). The parameters are the same as in Fig. 3, i.e., $C_H=0.5$ and $r_0/\xi=1$. The phenomenological capillary-wave theory does not yield a specific value for κ/σ_0. Here it is chosen such that this ratio has the same value as the one predicted by the present theory for large q. Only the present theory predicts the formation of a minimum of $\sigma_0(q)$.

tonian turns out to be qualitatively incorrect for describing the long-wavelength limit of capillary waves on fluid interfaces.

In principle $\sigma(q)$ can be inferred from the structure factor of a liquid-vapor interface (see below) as obtained from simulations. However, the accuracy of such data as presently available [24] does not allow one to extract a discernible deviation of the surface tension $\sigma(q)$ from its value σ_0 at $q=0$.

IV. PREDICTIONS FOR SCATTERING EXPERIMENTS

The momentum-dependent surface tension $\sigma_0(q)$ is experimentally accessible by x-ray or neutron scattering at grazing incidence which probe the two-point correlation function [25]

$$\langle\tilde{f}(\mathbf{q})\tilde{f}(\mathbf{q}')\rangle=G(\mathbf{q})(2\pi)^2\delta(\mathbf{q}+\mathbf{q}'), \tag{4.1}$$

where $\mathbf{q}$ is the lateral momentum transfer. Within the Gaussian approximation one has

$$G_0(\mathbf{q})=\frac{k_BT}{\Delta\rho mG(1-2\delta_Hq^2)+\sigma_0(q)q^2}. \tag{4.2}$$

This means that the analysis of the *diffuse* scattering intensity around the specular beam of x rays or neutrons, which are totally reflected at the liquid-vapor interface, allows one to retrieve the full functional form of $\sigma(q)$ whose Gaussian approximation is given by $\sigma_0(q)$ [Eq. (3.11) and Figs. 3–5]. [However, one should keep in mind that this diffuse scattering intensity in addition contains contributions which stem for the fluctuating semi-infinite liquid phase bounded by a planar, nonfluctuating liquid-vapor interface. These contributions must be separated off in order to obtain $G_0(\mathbf{q})$ in Eq. (4.2)]. The non-Gaussian contributions to $\sigma(q)$ give rise to a temperature dependence, which goes beyond that induced by the temperature dependences of the intrinsic density profiles $\rho_0(u)$ and $\rho_H(u)$ and of the direct correlation function, to a more complicated dependence on the gravity constant G and to a modification of the momentum dependence. Prelimary results indicate that the central results presented above for $\sigma_0(q)$ in systems with long-ranged forces remain valid for $\sigma(q)$ [26], in particular the singularity of $\sigma(q)$ at $q=0$, as well as the presence of a local maximum at $q=0$ and of a global minimum at $q_{\min}>0$.

From Eqs. (2.27), (2.28), and (3.27) and due to the normalization $\int_{-\infty}^{\infty}dx\overline{\rho}_H(x)=1$ one finds

$$\delta_H=C_H\xi^2. \tag{4.3}$$

Thus from studying the momentum dependence of the gravity term in Eq. (4.2), which can be varied independently, e.g., by changing the isotopic composition of the fluid, one can infer the amplitude C_H directly and independently. This is very useful because at present there is no reliable theoretical value for C_H available, but this value enters sensitively into the expression for $\sigma_0(q)$ at various places. In particular, the comparision with the large q behavior $\sigma(q\to\infty)=\kappa q^2$ [Eq. (3.45)] can provide an interesting consistency check.

In recent experiments the *lateral* surface correlations of an oil-water interface [27] and of the liquid-vapor interface of ethanol [28] and water [29,30] were studied using x-rays under grazing incidence [31]. So far these experiments have been focused on the very vicinity of the specular beam probing the *leading* q dependence for $q\to0$ in Eq. (4.2). These experiments demonstrated that this leading behavior $\sim\sigma_0(0)q^2$ is in agreement with the expected roughening of the fluid interface in the limit of microgravity, i.e., $G\to0$. Our present theory is in accordance with these findings. However, the main thrust of the present analysis predicts a nontrivial behavior of the *next-to-leading* term $\sim q^4\ln q$ in the denominator of $G_0(q)$ [Eq. (4.2)]. Its nonanalytic behavior and its sign contain the fingerprints of the dispersion forces on the fluctuations at the fluid interface. Although the measured off-specular diffuse x-ray intensities of a bare water surface are not inconsistent with a constant surface tension σ_0 [29,30], the data for large values of q are too noisy as to allow one to analyze them in terms of a momentum-dependent surface tension. Nonetheless, there are first hints that at larger values of q the scattered intensity is larger than the one corresponding to Eq. (4.2) for a constant σ_0 [30]. This observation means that $\sigma_0(q)$ decreases as a function of q, in accordance with the present theory.

Recently, by using small-angle neutron scattering in the *bulk* the expected nonanalytic q^3 momentum dependence in the static structure function of simple liquids as induced by dispersion forces has been confirmed experimentally for Ar [32](a), Kr [32](b), and Xe [32](c). The present theory predicts its counterpart $\sim q^2\ln q$ at fluid *interfaces*. The bulk experiments revealed [32] that the strength of the bulk singularity $\sim q^3$ is determined by the sum of the long-ranged interaction given by the dipole-dipole dispersion energy plus

a triple-dipole contribution of the Axilrod-Teller type. Concerning the quantitative comparison between future experiments at interfaces with the present theory one should be prepared to include also three-body interactions not yet covered by Eq. (2.2). The three-body interactions are expected to influence the density dependence of $\sigma_0(q)$ but not its temperature and momentum dependence [32]

Since it is a demanding experimental task to determine $\sigma(q)$ from the diffuse scattering of x rays and neutrons at grazing incidence, it is worthwhile to note that with reduced experimental efforts one is able to infer at least averaged informations about $\sigma(q)$. Reflectivity ($i=0$) and ellipsometry ($i=1$) experiments allow one to determine the moments [23,28,33–38]

$$F_i^2 = \int_0^{q_{\max}} dq q^{1+i} G(q). \tag{4.4}$$

Since $\sigma_0(q\to\infty)$ increases as κq^2 with $\kappa>0$, one has $G_0(q\to\infty)\sim q^{-4}$ so that in Eq. (4.4) the momentum cutoff $q_{\max}=1/r_0$ can be replaced by infinity without encountering a convergence problem even within the Gaussian approximation. This improves the theoretical results of Ref. [14] which are valid only for small q and thus cannot capture the increase of $\sigma_0(q)$ for large q. Although it is convenient to be able to remove the cutoff $q_{\max}$ in Eq. (4.4) and thus to get rid of an additional fitting parameter, one has to keep in mind that on physical grounds the theoretical description of interface fluctuations in terms of local height variables requires the cutoff $q_{\max}$ conceptually. Therefore in analyzing such experiments one should test the importance of the contribution $\int_{q_{\max}}^{\infty} dq\, q^{1+i} G(q)$ for the interpretation of the data. Also for this reason it would be very important to probe $G(q)$ directly as described by Eqs. (4.1) and (4.2) because the interpretation of the diffuse scattering intensity does not require a momentum cutoff. This would not only provide much more detailed information but it would also allow one to assess the importance of the aforementioned contributions to $G(q)$ for large values of q.

V. SUMMARY

We have obtained the following main results.

(1) Based on density functional theory for inhomogeneous liquids we have derived an effective Hamiltonian for gas-liquid interfaces in simple fluids which takes into account both the presence of long-ranged dispersion forces in the fluid and the smooth variation of the intrinsic density profile [Eq. (2.11)].

(2) In order to achieve an optimal implementation of the concept of the intrinsic density profile we have introduced normal coordinates (Fig. 2). Close to the interface position the distortion of the planar intrinsic density profile due to curvature is taken into account [see Eq. (2.17)].

(3) The approach described in (2) allows one to derive the explicit functional dependence of the effective interface Hamiltonian $\mathcal{H}[f(\mathbf{R})]$ on the interface configuration $f(\mathbf{R})$ (Sec. II C). $\mathcal{H}[f(\mathbf{R})]$ consists of local functionals, due to the gravity contribution and due to the curvature-induced distortion of the intrinsic density profile and of nonlocal functionals stemming from the nonzero range of the interaction potential between the fluid particles [Eq. (2.24)].

(4) Within the Gaussian approximation $\mathcal{H}[f(\mathbf{R})]$ can be expressed in terms of a momentum-dependent surface tension $\sigma_0(q)$ [Eqs. (3.10) and (3.11)] whose behavior is shown in Fig. 3. Its salient features for fluids governed by dispersion forces are a local maximum at $q=0$ which is attained linearly $\sim q$ followed, via a crossover, by a singularity $\sim q^2 \ln q$, a global minimum at $q_{\min}>0$, and an increase $\sim q^2$ for large q. The latter property is caused by the distortion of the intrinsic density profile due to curvatures [Eq. (2.17)] and renders an upper momentum cutoff in correlation functions of $f(\mathbf{R})$ effectively redundant. In systems governed by short-ranged forces $\sigma_0(q)$ is analytic and the global minimum may be shifted to $q=0$. These results differ qualitatively from those obtained from the phenomenological capillary wave theory. This means that the Helfrich Hamiltonian is not applicable for describing fluid interfaces (Fig. 5).

(5) The appearance of the minimum of the momentum-dependent surface tension is most pronounced near the triple point of the fluid. Upon approaching T_c the depth of the minimum vanishes $\sim t^{1-a}$, $t=(T_c-T)/T_c\to 0$, and the position of the minimum shifts towards $q=0$ proportional to $t^{a/2}$ where the exponent $a=1,2$ depends on the amplitude C_H [Eqs. (2.17) and (3.27)] of the distortion of the intrinsic density profile due to curvatures (see Fig. 4). Near T_c as a function of $q\xi$, where ξ is the bulk correlation length, $\sigma_0(q)/\sigma_0(0)$ reduces to an analytic limiting function [Eq. (3.61) and Fig. 3(a)].

(6) The momentum-dependent surface tension can be probed experimentally either directly through the diffuse scattering intensity around the specular beam of totally reflected x rays or neutrons [Eqs. (4.1) and (4.2)] or indirectly via averaged moments obtained from reflectivity or ellipsometry experiments [Eq. (4.4)].

ACKNOWLEDGMENT

It is a pleasure for us to thank M. Napiórkowski for numerous discussions.

[1] *Fluid Interfacial Phenomena*, edited by C.A. Croxton (Wiley, Chichester, 1986).

[2] *Liquids at Interfaces*, edited by J. Chavrolin, J.F. Joanny, and J. Zinn-Justin, Les Houches Summer School Lectures, Session XLVIII (Elsevier, Amsterdam, 1990).

[3] G. Pétré and A. Sanfeld, *Capillarity Today* (Springer, Berlin, 1991).

[4] J.D. van der Waals, Verh. K. Ned. Akad. Wet. Afd. Natuurk. Reeks **1**, 8 (1893); Z. Phys. Chem., Stoechiom. Verwandtschaftsl. **13**, 657 (1894); an English translation can be

found in J.S. Rowlinson, J. Stat. Phys. **20**, 197 (1979).
[5] F.P. Buff, R.A. Lovett, and F.H. Stillinger, Phys. Rev. Lett. **15**, 621 (1965).
[6] D. Jasnow, Rep. Prog. Phys. **47**, 1059 (1984).
[7] J.D. Weeks, J. Chem. Phys. **67**, 3106 (1977).
[8] D. Bedeaux and J.D. Weeks, J. Chem. Phys. **82**, 972 (1985).
[9] R. Evans, in *Liquids at Interfaces*, [2], p. 3.
[10] S.M. Thompson, K.E. Gubbins, J.P.R.B. Walton, R.A.R. Chantry, and J.S. Rowlinson, J. Chem. Phys. **81**, 530 (1984); M.P.A. Fisher and M. Wortis, Phys. Rev. B **29**, 6252 (1984); J.R. Henderson and J.S. Rowlinson, J. Phys. Chem. **88**, 6484 (1984); D.J. Lee, M.M. Telo da Gama, and K.E. Gubbins, J. Chem. Phys. **85**, 490 (1986); D. Oxtoby and R. Evans, *ibid.* **89**, 7521 (1988); X.C. Zeng and D.W. Oxtoby, *ibid.* **95**, 5940 (1991); G. Gompper and S. Zschocke, Phys. Rev. A **46**, 4836 (1992); Europhys. Lett. **18**, 731 (1991); V. Romero-Rochín, C. Varea, and A. Robledo, Physica A **184**, 367 (1992); Phys. Rev. A **44**, 8417 (1991); M.J.P. Nijmeijer, C. Bruin, A.F. van Woerkom, A.F. Bakker, and J.M.J. van Leeuwen, J. Chem. Phys. **96**, 565 (1992); E.M. Blokhuis and D. Bedeaux, Mol. Phys. **80**, 705 (1993); E.M. Blokhuis and D. Bedeaux, Heterog. Chem. Rev. **1**, 55 (1994); Mol. Phys. **80**, 705 (1993); Physica A **184**, 42 (1992); J. Chem. Phys. **95**, 6986 (1991); S.M. Osman, J. Phys.: Condens. Matter **6**, 6965 (1994); I. Hadjiagapiou, *ibid.* **6**, 5303 (1994); **7**, 547 (1995); V. Talanquer and D. Oxtoby, J. Chem. Phys. **100**, 5190 (1994); A. Robledo and C. Varea, Mol. Phys. **86**, 879 (1995); C. Varea and A. Robledo, *ibid.* **85**, 477 (1995); T. Bieker and S. Dietrich, Physica A **252**, 85 (1998); **259**, 466 (1998).
[11] F.B. Buff, J. Chem. Phys. **19**, 1591 (1951); **23**, 419 (1955); J.S. Rowlinson, J. Phys.: Condens. Matter **6**, A1 (1994); M. Iwamatsu, Chin. J. Phys. **33**, 139 (1995); M. Baus and R. Lovett, J. Chem. Phys. **103**, 377 (1995); J.W.P. Schmelzer, I. Gutzow, and J. Schmelzer, Jr., J. Colloid Interface Sci. **178**, 657 (1996); A. Laaksonen and R. McGraw, Europhys. Lett. **35**, 367 (1996); V.I. Kalikmanov, Phys. Rev. E **55**, 3068 (1997).
[12] W. Helfrich, Z. Naturforsch. C **28**, 693 (1973).
[13] F. David, in *Statistical Mechanics of Membranes and Surfaces*, edited by D. Nelson, T. Piran, and S. Weinberg (World Scientific, Singapore, 1989).
[14] (a) M. Napiórkowski and S. Dietrich, Phys. Rev. E **47**, 1836 (1993); (b) Z. Phys. B **89**, 263 (1992); (c) S. Dietrich and M. Napiórkowski, Physica A **177**, 437 (1991); (d) Z. Phys. B **97**, 511 (1995).
[15] R.K.P. Zia, Nucl. Phys. B **251** [FS13], 676 (1985).
[16] D.G. Triezenberg and R. Zwanzig, Phys. Rev. Lett. **28**, 1183 (1972).
[17] R. Evans, Adv. Phys. **28**, 143 (1979); in *Fundamentals of Inhomogeneous Fluids*, edited by D. Henderson (Dekker, New York, 1992), p. 85.
[18] Starting from a Lennard-Jones interaction potential $W(r)=\epsilon[(\sigma/r)^{12}-(\sigma/r)^{6}]$ the standard separation into $w_s(r)$ and $w(r)$ according to WCA [J.D. Weeks, D. Chandler, and H.C. Andersen, J. Chem. Phys. **54**, 5237 (1971)] leads to $w_{\mathrm{WCA}}(r \geqslant 2^{1/6}\sigma)=W(r)$ and $w_{\mathrm{WCA}}(r \leqslant 2^{1/6}\sigma)=-\epsilon$. The resulting nonanalyticity of $w_{\mathrm{WCA}}(r)$ at $r=2^{1/6}\sigma$ prevents an analytic evaluation of certain integrals involving $w(r)$. Our choice in Eq. (2.2) reduces to $w_{\mathrm{WCA}}(r)$ for $r\to\infty$ with $r_0=\sigma$ and $w_0=\epsilon$ and resembles closely $w_{WCA}(r)$ for small r [$w(r=0)=w_{\mathrm{WCA}}(r=0)$]; furthermore, $w(r)$ has the advantage that it is analytic and thus facilitates our following analysis. This advantage outweighs the fact that Eq. (2.2) deviates slightly from the standard WCA approach.
[19] D.E. Sullivan, Phys. Rev. B **20**, 3991 (1979); J. Chem. Phys. **74**, 2604 (1981).
[20] S. Dietrich and M. Napiórkowski, Phys. Rev. A **43**, 1861 (1991), and references therein.
[21] A.O. Parry and C.J. Boulter, J. Phys.: Condens. Matter **6**, 7199 (1994).
[22] A.O. Parry and C.J. Boulter, Physica A **218**, 77 (1995); **218**, 109 (1995); A.O. Parry and P.S. Swain, *ibid.* **250**, 167 (1998).
[23] J. Meunier, J. Phys. (Paris) **48**, 1819 (1987).
[24] J. Stecki, J. Chem. Phys. **108**, 3789 (1998); **107**, 7967 (1997); **103**, 9763 (1995); E.M. Blokhuis, J. Groenewold, and D. Bedeaux, Mol. Phys. **96**, 397 (1999).
[25] S. Dietrich and A. Haase, Phys. Rep. **260**, 1 (1995).
[26] K. R. Mecke and S. Dietrich (unpublished).
[27] B.R. McClain, D.D. Lee, B.L. Carvalho, S.G.J. Mochrie, S.H. Chen, and J.D. Lister, Phys. Rev. Lett. **72**, 246 (1994).
[28] M.K. Sanyal, S.K. Sinha, K.G. Huang, and B.M. Ochs, Phys. Rev. Lett. **66**, 628 (1991).
[29] M. Fukuto, R.K. Heilmann, P.S. Pershan, J.A. Griffiths, S.M. Yu, and D.A. Tirrell, Phys. Rev. Lett. **81**, 3455 (1998).
[30] C. Fradin, A. Braslau, D. Luzet, M. Alba, C. Gourier, J. Daillant, G. Grübel, G. Vignaud, J.F. Legrand, J. Lal, J.M. Petit, and F. Rieutord, Physica B **248**, 310 (1998); C. Fradin and J. Daillant (private communication).
[31] J. Daillant, K. Quinn, C. Gourier, and F. Rieutord, J. Chem. Soc., Faraday Trans. **92**, 505 (1996); A. Braslau, P.S. Pershan, G. Swislow, B.M. Ocko, and J. Als-Nielsen, Phys. Rev. A **38**, 2457 (1988); S.K. Sinha, E.B. Sirota, S. Garoff, and H.B. Stanley, Phys. Rev. B **38**, 2297 (1988); J. Daillant and O. Belorgey, J. Chem. Phys. **97**, 5824 (1992).
[32] (a) R. Magli, F. Barocchi, P. Chieux, and R. Fontana, Phys. Rev. Lett. **77**, 846 (1996); (b) F. Formisano, C.J. Benmore, U. Bafile, F. Barocchi, P.A. Egelstaff, R. Magli, and P. Verkerk, *ibid.* **79**, 221 (1997); (c) F. Formisano, F. Barocchi, and R. Magli, Phys. Rev. E **58**, 2648 (1998).
[33] P.S. Pershan, Faraday Discuss. Chem. Soc. **89**, 231 (1990).
[34] R. Braslau, M. Deutsch, P.S. Pershan, A.H. Weiss, J. Als-Nielsen, and J. Bohr, Phys. Rev. Lett. **54**, 114 (1985).
[35] J.S. Huang and W.W. Webb, J. Chem. Phys. **50**, 3677 (1969).
[36] E.S. Wu and W.W. Webb, Phys. Rev. A **8**, 2065 (1973).
[37] D. Beaglehole, Phys. Rev. Lett. **58**, 1434 (1987).
[38] D. Bonn and G.H. Wegdam, J. Phys. I **2**, 1755 (1992).